

ACADEMIC STUDIES IN GEOSCIENCE



Editor
ADNAN DÖYEN



BIDGE Publications

ACADEMIC STUDIES IN GEOSCIENCE

Editor: ADNAN DÖYEN

ISBN: 978-625-372-881-6

1st Edition

Page Layout By: Gozde YUCEL

Publication Date: 18.12.2025

BIDGE Publications

All rights reserved. No part of this work may be reproduced in any form or by any means, except for brief quotations for promotional purposes with proper source attribution, without the written permission of the publisher and the editor.

Certificate No: 71374

All rights reserved © BIDGE Publications

www.bidgeyayinlari.com.tr - bidgeyayinlari@gmail.com

Krc Bilişim Ticaret ve Organizasyon Ltd. Şti.

Güzeltepe Mahallesi Abidin Daver Sokak Sefer Apartmanı No: 7/9 Çankaya /
Ankara



Contents

IRON ORE DEPOSITS IN AFGHANISTAN AND THE HAJI-GAK IRON ORE DEPOSIT	4
FETULLAH ARIK	4
ALPER DÜLGER	4
GÜRSEL KANSUN	4
COPPER DEPOSITS IN AFGHANISTAN AND THE BALKHAB COPPER DEPOSIT	32
GÜRSEL KANSUN	32
ALPER DÜLGER	32
FETULLAH ARIK	32
SMALLER FORAMINIFERAL ASSEMBLAGE OF THE BASHKIRIAN SUCCESSION IN THE HADİM NAPPE (SOUTHERN TÜRKİYE) AND ITS BIOSTRATIGRAPHIC CORRELATION	70
MELİKAN AKBAŞ	70
CENGİZ OKUYUCU	70

IRON ORE DEPOSITS IN AFGHANISTAN AND THE HAJI-GAK IRON ORE DEPOSIT

**FETULLAH ARIK¹
ALPER DÜLGER²
GÜRSEL KANSUN³**

Introduction

Afghanistan has huge mineral and energy resources that could contribute greatly to the country's mining, industry, foreign trade and economy. Lots of important economically exploitable level metallic ore deposits (iron, copper, gold, silver, lead, zinc, chromite, cobalt, molybdenum, aluminum, tin, lithium, mercury, wolfram, rare earth elements, etc.), industrial raw mineral deposits (sulfur, asbestos, gypsum, halite, barite, Na-sulphate, Na-Carbonate, graphite, quartz, clay, mica, olivine, serpentine, talc, magnesite, etc.), natural building stones (limestone, marble, dolomite, clay, gravel, sand, etc.), energy resources (coal, oil shale, oil and natural

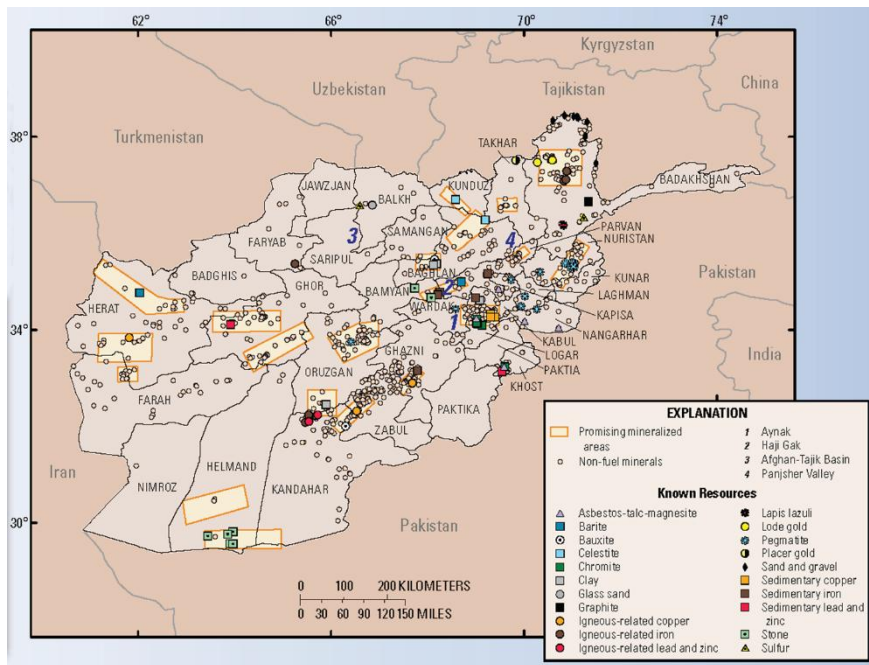
¹ Professor, Konya Technical University, Geological Engineering, 0000-0003-0833-7778

² Research Assistant, Konya Technical University, Geological Engineering, 0000-0003-3380-7663

³ Assistant Professor, Konya Technical University, Geological Engineering, 0000-0002-4581-6076

gas), and economic-sized high-quality gemstones (beryl, emerald, tourmaline, ruby, lapis lazuli and red garnet, aragonite, amethyst, kunzite, spodumene, aquamarine, etc.) are there in the Country. In addition, almost all of Afghanistan's oil and natural gas reserves are in the Amu Darya Basin in the west of the country and the Afghan-Tadjik Basin in the east of the country, and it is known that the use of these resources is quite limited (Figure 1).

Figure 1 Mineral resources of Afghanistan



Source: (AGS, 1967)

Afghanistan has billion tons of high-quality estimated iron reserves. Iron deposits occur along a line from Badakhshan to Herat extends several hundred km (Badakhshan, Panjshir, Ghorband, Bamyan, Hajigak, Behsood, Yakowlang, Lal o Sarjangal, Ghore, and Ghorian). The Haji-Gak iron deposit in Bamyan Province is the best known and largest iron oxide deposit in Afghanistan.

However Afghanistan has very rich mineral and energy resources, these resources have not yet been sufficiently scientifically researched. Country's long-term economic growth, it is crucial that underground resources be explored in more detail using comprehensive scientific methods, the general characteristics of mineral deposits be revealed, and their exploitation and integrating into the economy are crucial.

Geology of Afghanistan

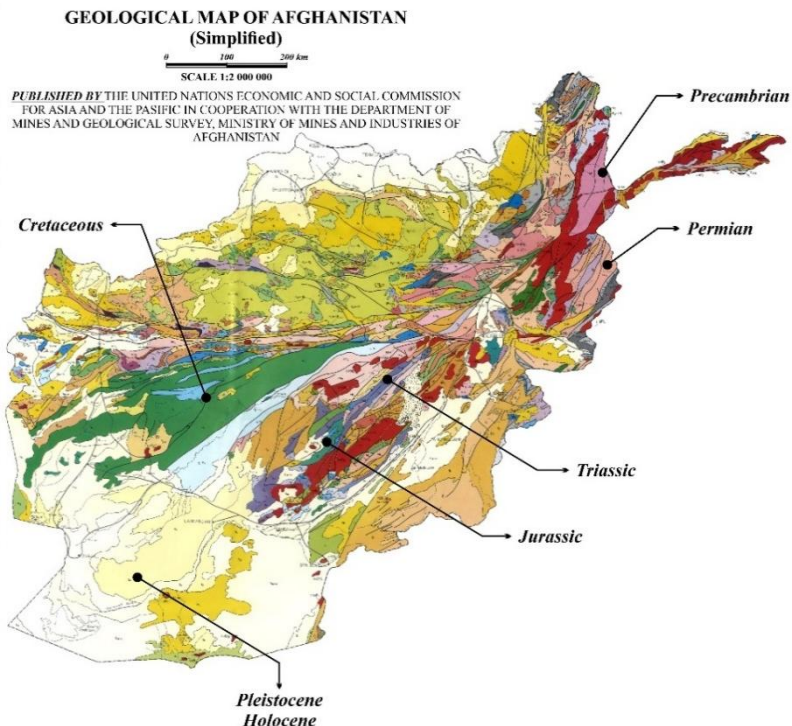
Afghanistan, located in the tectonically active Alpine-Himalayan orogenic belt formed by the collision of the Indian and Arabian plates with the Eurasian plate in Central Asia during the Late Paleogene, has a highly complex geological structure. Metamorphic, magmatic and sedimentary rocks formed in different stages from the Precambrian to the present day are exposed in the country. While older rock units are found in the central and eastern parts of the country, younger units are found in the border regions in the north and in large areas in the south. There was different geological activity in each zone which resulted in formation of very rich mineral assemblages (Figure 2).

As the Eurasian continent emerged 65 million years ago, multiple periods of deformation shattered the crust around Afghanistan (Kansun & Afzali, 2022). Northern portion is part of Eurasia Plate and the south is made up of accreted blocks of Gondwana Land. Coal and oil/gas are found on the Eurasian plate.

Afghanistan consists of a complex assemblage of areas mostly originating from Gondwana, that was added to the southern margin of Eurasia before and during the collision of the Indo-Eurasian plates. These areas are divided into three separate tectonic zones (Figure 2; Figure 3).

- 1) **Afghan-Tadjik Block** lies north of the Harirod-Panjshir fault system in the north consists of fixed blocks, and since the Paleozoic, these blocks have been part of the Eurasian continent.
- 2) **The Katawaz Basin** the front fold and thrust belts which were a major bending basin in the southeast represents the northwestern continental margin of the Indian plate.
- 3) **Afghan Center Blocks** (Farah and Helmand Blocks) that is NE-SW extension tectonic blocks.

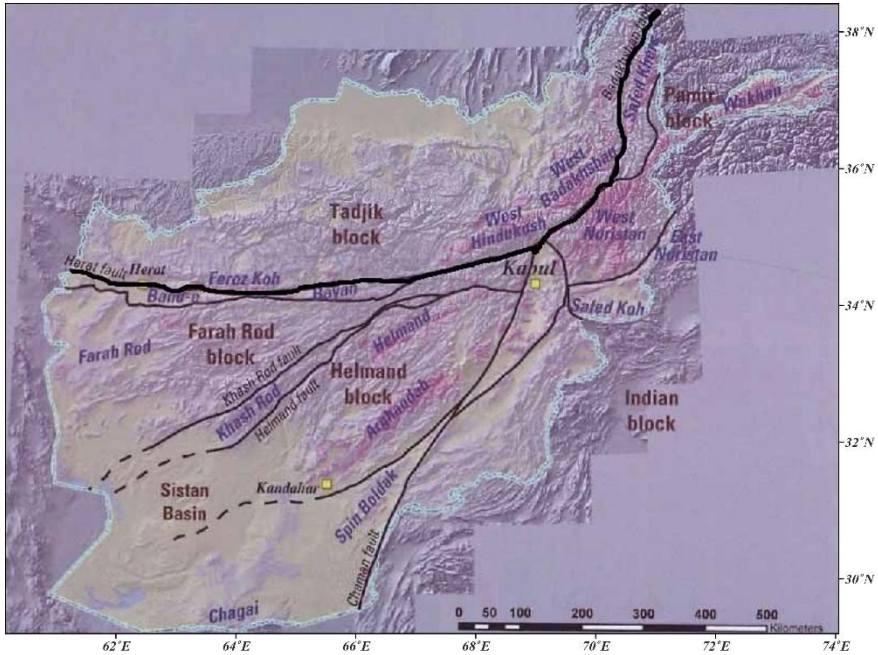
Figure 2 Geological map of Afghanistan (Compiled on the basis of the draft geological map of Afghanistan at a scale 1:2.000.000 prepared by department of mines and geological survey of the ministry of mines and industries of Afghanistan for the ESCAP mineral atlas).



Source: (ESCAP, 1995)

The blocks collided with Eurasia during the Mesozoic and Early Cenozoic. Each block is separated by deep seated faults.

Figure 3 Tectonic outlines of Afghanistan, major structural blocks, plutonic belts and faults



Source: (Shareq et al., 1977)

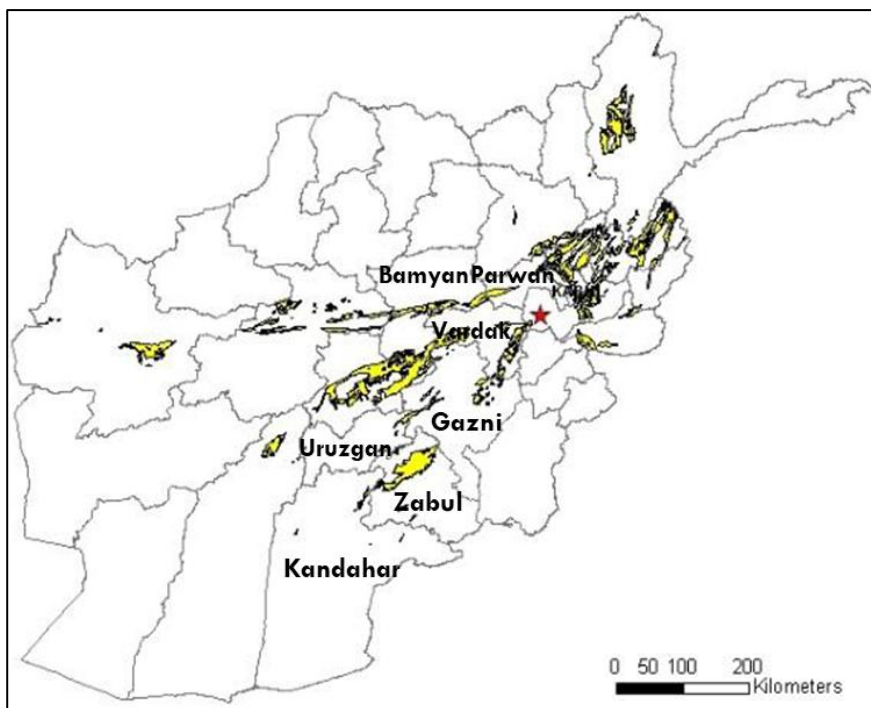
Iron Deposits of Afghanistan

Afghanistan has world class iron deposits. Iron deposits occur along a line from Badakhshan to Herat. Extends several hundred km (Badakhshan, Panjshir, Ghorband, Bamyan, Hajigak, Behsood, Yakowlang, Lal o Sarjangan, Ghore, and Ghorian). Reserves are estimated at billions of tons of high-quality iron containing a very attractive mixture of elements, Mo, Ti, V, and Mn (ESCAP, 1995; AGS, 2011; Shroder et al., 1992).

Iron deposits found in sedimentary rocks in Afghanistan are mostly found in Proterozoic metasedimentary and metavolcanic-

metasedimentary rocks (Peters et al., 2007). From the Late Paleozoic to the Cenozoic, the formation of an oolitic iron stone mineral in sedimentary rocks is also known (Nishiwaki, 1970). Sedimentary iron deposits also occur along from Badakhshan to Herat from NE to W of country. In addition, there are lots of sedimentary iron deposits from east to center of Afghanistan such as Nuristan, Panjher, Parwan, Kapisa, Lanhgman, Bamyan, Maydan, Wardak, Kabul, Nanganhar, Daykundi, Ghazni, Zabul and Helmand, Hematite vein deposits are also found in Proterozoic, Permian, and Oligocene rocks (Figure 4).

Figure 4 Sedimentary iron deposits of Afghanistan



Source: (Peters et al., 2007)

The main ore minerals in sedimentary iron deposits in Afghanistan are hematite, magnetite and goethite, with smaller

amounts of martite. The metallogenic age, mineralogy, textures and dimensions of the deposits make them compatible with various model BIF (banded iron formations) types, such as Superior type banded iron formations (Cannon, 1986a) formed in the passive continental shelves or intracratonic basin and Algoma type banded iron formations (BIF) (Cannon, 1986b) formed near volcanic arcs and spreading centers), and iron oxide copper-gold (IOCG) deposits (Cox, 1986; Haynes, 2000; Hitzman, 2000). More detailed investigations have shown that the Algoma iron-type deposit most closely resembles the Haji-Gak iron-type deposit, which hosts volcanogenic iron-bearing sequences predominantly of Archaean or Proterozoic age. Similar to the Haji-Gak iron-type deposit, the Algoma iron-type deposit is characterized by micro- and mesoband lensoids extending along a distinct strike distance of more than 10 kilometers and less than 50 meters thick (Bekker et al., 2010). The Algoma iron-type deposits are generally associated with mafic to felsic submarine volcanic rocks and deep-water clastic and volcanoclastic sediments. The rock textures include pillow greenstone, intermediate to felsic tuff and agglomerate, and poorly sorted clastic sediments interbedded with deep-water greywacke and mudstone (Cannon, 1986a; Cannon, 1986b).

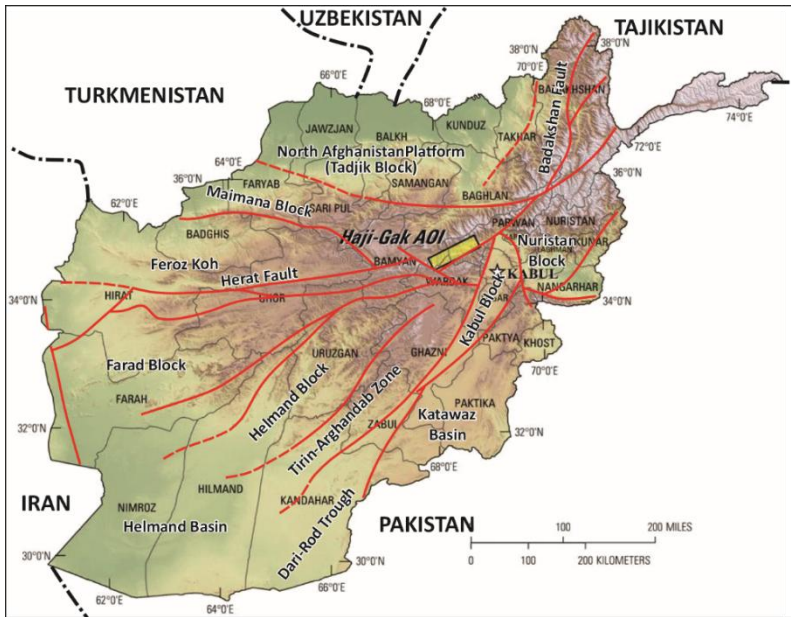
Other important iron deposits in Afghanistan are mostly in iron skarn bodies around Oligocene intrusive bodies in Kandahar and Badakshan Provinces. Some geologists believe that the sediments found in the Proterozoic are the products of contact metamorphism around Oligocene intrusive bodies (Peters et al., 2007).

Most iron deposits, including the Haji-Gak iron deposit and its associated deposits, are located along a tectonized region along the Herat Fault line in central Afghanistan (Figure 3), (Renaud et al., 2011).

Haji-Gak Iron Deposits

The Haji-Gak iron deposit is located in the northeastern part of Afghanistan. It is approximately 100 km W of Kabul. The Haji-Gak iron deposits lies in parts of Parwan and Wardak Provinces and some parts of Bamyan, Beshud, Ghorband, Hisa-i-Awal, Markazi, Shekh Ali, Shibar and Surkh-i-Parso Districts (Figure 5).

Figure 5 Tectonic map of Afghanistan showing major blocks and faults and location of Hajigak Iron deposits



Source: Modified after (Livo & Giles, 2011)

The Haji-Gak Fe area covers an area of 2,079 km² and it is divided into 3 sub-areas (Figure 6; Figure 7); Haji-Gak prospect sub area (180 km²), NE Haji-Gak sub area (381 km²) and Farenjal subarea (557 km²).

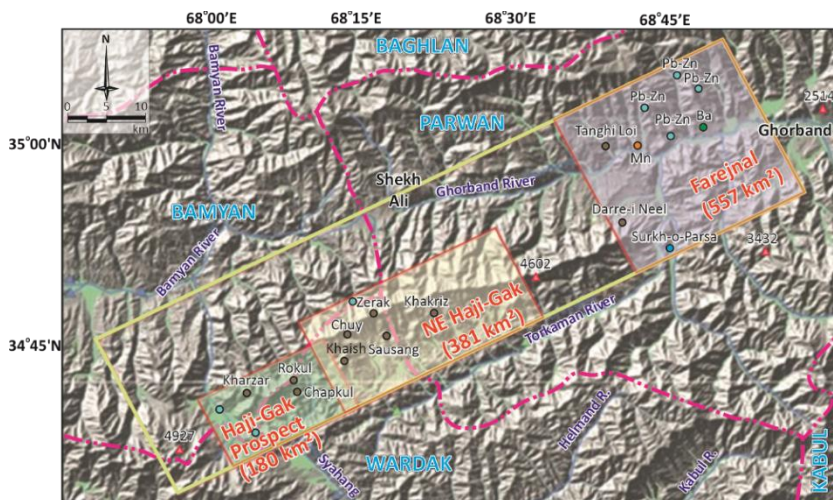
Haji-Gak iron field is located in the vicinity of Turkman Mountains, which is the western extension of Hindu Kush Range. The topography of Haji-Gak iron field is generally controlled by a

mountain range trending E-NE. The highest elevation here is 4602 m. A NW-trending mountain range is observed in the SW corner of Haji-Gak Fe field. The highest peak here is 4927 m. The Ghorbank River in the N, the Torkaman River in the S, a tributary of Bamyán River in the SW and the Sayang River are important rivers. The elevation difference between the river valleys and the peaks of the mountains is about 1900 m.

The Haji-Gak iron deposit (prospect subfield) in Bamyán Province is the best known and largest iron oxide deposit in Afghanistan. Besides the Haji-Gak iron prospect in the Haji-Gak Iron field Khaish, Kharzar, Chuy, Rokul, Chapkul, Zerak, Khakriz, Sausang, Darre-i Neele and Zerak are important iron deposits.

In the SW of the Haji-Gak iron deposits the formation of Mangasak Fe in Wardak Province and a manganese formation in Uruzgan Province NE.

Figure 6 Haji-Gak iron deposits and sub basins of Afghanistan



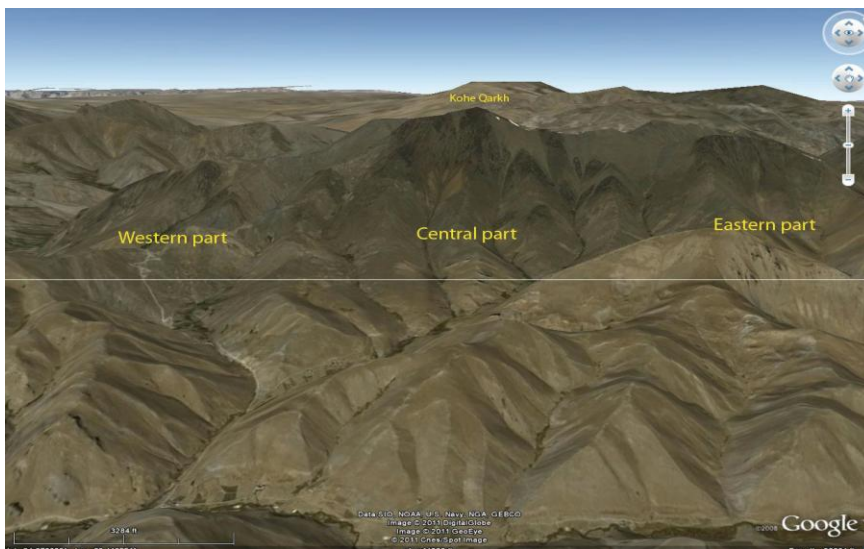
Source: Modified after Renaud et al. (2011)

The mangasak Fe formation is located in a 1200 m long and 50 - 100 m wide carbonate zone containing scattered, nodular and

veiny magnetite, between layers of gneiss and schists of Proterozoic age (Karapetov, Stazhilo-Alekseyev & Kotchetkov, 1970).

The unnamed manganese formation consists of 1.5 x 7 m lenses within Neoproterozoic chert marl rocks (Shareq et al., 1977). The Farejnal area has not only iron formations also important lead, zinc, barite and manganese deposits.

Figure 7 Location of the three sections of the Haji-Gak iron deposit as viewed from SW on Google Earth



Source: after Renaud et al. (2011)

Stratigraphy of Haji-Gak Iron Deposit

The area including Haji-Gak iron deposits consist of metavolcanic and metasedimentary rocks of Middle to Late Proterozoic age as well as Paleozoic and Tertiary rocks (Shareq et al., 1977; Peters et al., 2007) (Figure 8; Figure 9). However, (Bouladon & de Lapparent, 1975) suggested that the Haji-Gak iron deposit was formed in the Early Paleozoic (probably Silurian to Lower Devonian) based on its stratigraphic position in the Awband

Formation, over metamorphosed Proterozoic gneiss and under Late Devonian fossil-bearing formations.

The Mesoproterozoic Jawkol formation, which is located at the base and consists of gray crystallized limestones and dolomite marbles, interbedded with dark gray crystalline schists and light colored quartzites, has undergone metamorphism in the amphibolite facies. This unit is observed in the NW part of the area.

The Neoproterozoic Kab formation and the overlying Awband formation consist of metavolcanic and metasedimentary rocks interpreted to have accumulated in the marine basin, and they form the Qala Series (Kusov, Smirnov & Reshetnyak, 1965a).

The Kab formation consists of dark gray sericite schists, felsic volcanic rocks, marbles and phyllites and porphyrite lenses, interpreted as metamorphosed terrestrial metasedimentary and metavolcanic rocks (Kusov, Smirnov & Reshetnyak, 1965a).

The Awband formation contains quartz-sericite schists and quartz-chlorite-sericite schists, quartzite, along with cherts and dolomitic and calcitic marbles with interbeds of metavolcanic rocks. These rocks are metamorphosed to the greenschist facies. The Awband formation hosts most of the iron deposits, which are assumed to be sedimentary exhalative iron-rich fluids that formed lenses on the sea floor during periods of increased volcanic activity (Peters et al., 2007).

The Qala Series is overlain by the Neoproterozoic Green Schist formation, which consists of quartz-chlorite-sericite schist and quartz-chlorite schist, plagioporphry with sparse scapolite, and metavolcanic rocks locally cut by granodiorite of chlorite schists and quartz-sericite schists, with less iron mineralization.

In the SE of the Proterozoic rocks, limestones, conglomerates, sandstones and pelagic schists ranging from

Smirnov & Reshetnyak 1965a; Kusov, Smirnov & Reshetnyak, 1965b).

Upper Carboniferous Horzar (Kharzar) formation consisting of pelitic schists, quartz-rich schists, metasandstones, quartzites and metaconglomerates unconformably overlies the Haji-Gak formation. In the SW part of the area, Lower Cretaceous and younger cover rocks are observed unconformably overlies the older rocks.






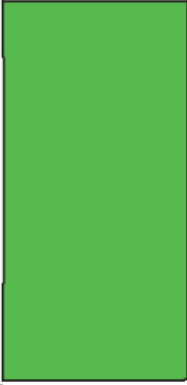

The lower part of the Lower Cretaceous rocks consists of red conglomerates, sandstones and limestones. Neogene rocks are gently dipping layers of red conglomerates and sandstones. The uppermost part of these young beds consists, in part, of rubble or gravel of fragmented iron-mineral rocks eroded from in-situ iron formations.

The Awband formation hosts most of the iron deposits, which are assumed to be sedimentary exhalative iron-rich fluids that formed lenses on the sea floor during periods of increased volcanic activity (Peters et al., 2007). The Haji-Gak iron deposit consists of a series of folded and faulted iron-rich lenses. The lenses are altered and contain cross-cutting iron veins. The iron-bearing rocks are extensively sericitized and silicified.

During the Cretaceous, displacement along the Herat fault zone juxtaposed Middle Proterozoic, Late Proterozoic and Upper Paleozoic rocks, and formed the NE-trending Haji-Gak anticline, which hosts iron deposits on its SE branch exposed within the Late Proterozoic units (Kusov, Smirnov & Reshetnyak, 1965b).

The dominant strike in the Haji-Gak deposit is NE and has a regional dip of 50° towards SE. The Haji-Gak iron deposits are located in the SW area (Haji-Gak Prospect subfield) and mineralization like known iron deposits is exposed along a high ridge to the NE (NE Haji-Gak subfield), and is cut by a fault at its NE end Farenjal subfield (Doebrich et al., 2006).

Figure 9 Stratigraphic columnar section of Haji-Gak iron deposits

Post-Jurassic cover		>600 m	Cretaceous, Neogene and Quaternary cover
Upper Carboniferous		>2500 m	Horzar Formation pelitic schists, quartz rich schists, sandstones, quartzites, conglomerates
Upper Devonian		900 m	Hajigak Formation limestones, conglomerates, sandstones, pelitic schists
Upper Proterozoic		700 m	Green Schist Formation quartz-chlorite-sericitic schists, quartz-chlorite schists, extrusives
		300–1000 m	Awband Formation quartz-sericitic schists, chlorite-sericitic schists, marbles, quartzites, extrusives, lenses of iron ores
		3500 m	Kab Formation quartz-sericitic schists, phyllites, marbles, altered extrusives lenses
		1000 m	Jawkol Formation crystalline schists, quartzites, silicified limestones and dolomites
Middle Proterozoic			

Source: (from Sutphin, Renaud & Drew (2011)) modified after (Kusov, Smirnov & Reshetnyak, 1965b)

Sub Areas of Haji-Gak Iron Deposits

The Haji-Gak Iron deposit is divided into 3 sub-areas, namely the Haji-Gak prospect sub-area, the NE Haji-Gak sub-area and the Farenjal sub-area.

Haji-Gak Prospect Sub Area

The Haji-Gak prospect subfield, which contains the best-known and most exposed iron oxide deposit in Afghanistan, is observed on Kohe Qarkh Hill, at an altitude of approximately 3840 m near the center of the deposit (Figure 10). This deposit is an outcropping, centered roughly on Kohe Qarkh and extending towards the NE about 11 km long.

The Haji-Gak ore deposit (prospect subfield) is more than 12 km long and more than 3 km wide. It contains 16 separate zones, some of which are 5 km long, 380 m wide, and extend 550 m downhill (Renaud et al., 2011).

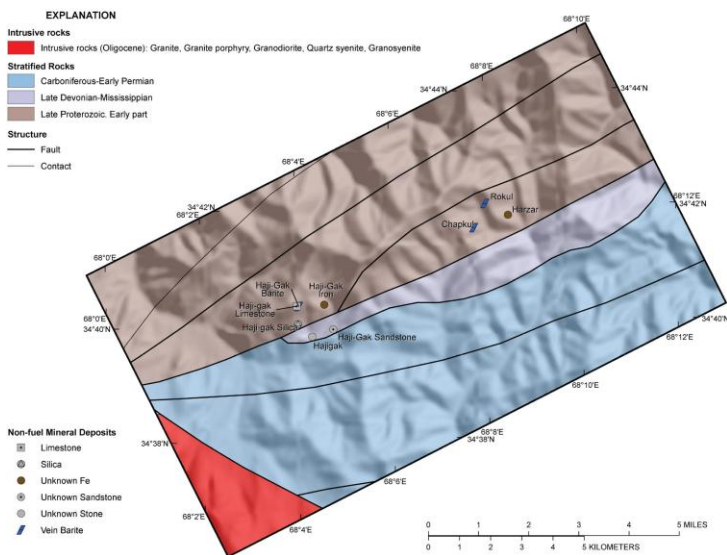
Iron mineralization is said to extend intermittently in an E-W belt more than 600 km from central Afghanistan (AGS, 2011; Orris & Bliss, 2002; Peters, 2007). The Haji-Gak prospect subfield iron deposit area is known for its complex magmatic activity, which spans a long period of time and includes both plutonic and volcanic rocks. Kusov, Smirnov & Reshetnyak (1965a) divided the plutonic rocks into 5 types;

- Serpentinites, which occur as thin (up to 5 m) dykes and sills in the Jawkol formation and consist of green schistose fine-grained rocks.
- Metadiabases, which occur as hypabyssal intrusions up to 1 km in diameter and are widespread among the Paleozoic rocks in the region. Kusov, Smirnov & Reshetnyak (1965a) suggested that the metadiabases and serpentinites were emplaced sometime after the Early Carboniferous and before the end of

the Triassic or the beginning of the Jurassic, when mafic and ultramafic magmatism ended and granitic magmatism began.

- Granitic plutons are widespread in the region where they cut the Upper Triassic formations and are covered by Middle Jurassic formations.
- Small granitoids occur in small massifs up to 600 m wide and 2,000 m long and in stocks of plagiogranite, granodiorite, quartz diorite and quartz diorite porphyry. Granites and small granitoid plutons may have the same source as the granitoid magmatic complex (Kusov, Smirnov & Reshetnyak, 1965a).
- The last type of plutonic rocks, alkali rocks, occur as sparse thin dykes and veins of keratophyres and stock-like bodies of metasomatic carbonatites up to 300 m in diameter. They seem to have been emplaced somewhat later or simultaneously with the small granitoids.

Figure 10 Known mineral occurrences in the Haji-Gak subarea



Source: from (Livo & Giles, 2011)

The Haji-Gak iron deposit surfaces along the S slopes of the mountains as rocky ridges along the NE-SW slope of the ridge crest (Fig 11a). Kusov, Smirnov & Reshetnyak (1965b) described 16 masses of in-situ iron mineralization and 4 masses of fragmented mineralized bulk materials at Haji-Gak. The original mineralized material in situ as confined to the Awband formation, which has a thickness of 1200 m and a length of about 12 km.

Mineralized masses are formed as tabular or lenticular masses, the direction and slope of which coincide with the predominant sinuous structure of the region. Mineralized masses are confined to the southern arm of a regional anticlinorium.

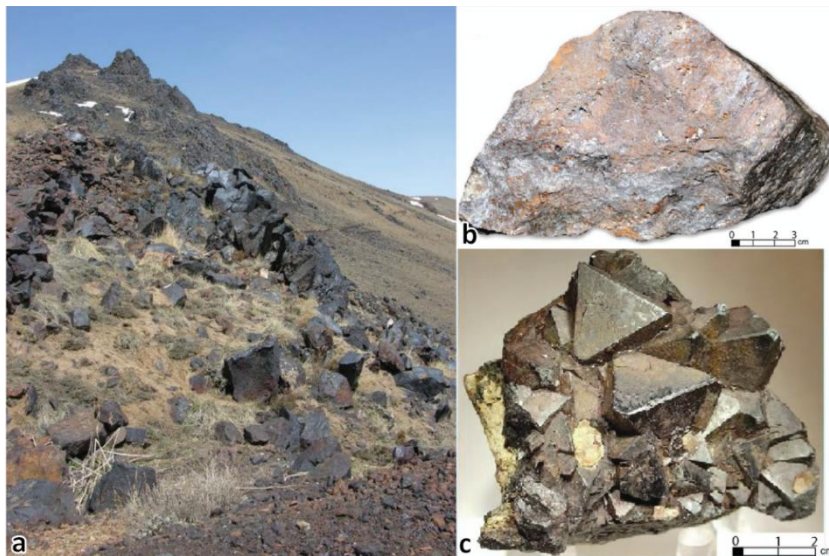
In the Haji-Gak subarea, iron ore is primary and oxidized. Up to 100 to 130 m below the existing surface, the mineralized material is partially or completely oxidized.

The primary ore (80% of the deposit by volume) is located below 130 m, consists mostly of magnetite (40–90%) and pyrite (2–35%) as well as hematite and martite, lesser amount of chalcopyrite and other sulfide minerals. Gangue minerals include carbonates (calcite, dolomite, siderite), barite, silicate minerals (quartz, chlorite and sericite) and contains an average of 61.3% iron by weight (Renaud et al., 2011). The primary ores are dense, fractured, steel-black in color and exhibit massive (Fig. 11a and b), massive-banded, and mottled textures with fine to medium and rare coarse-grained, xenomorphic, and idiomorphic (Fig 11 c) grains.

Primary semioxidized ore represented by hydrogoethite-semimartite, hydrogoethite-hematite-semimartite, and carbonate-semimartite ores. Fragmental ores contain only hydrogoethite-semimartite ore.

The remaining 20 vol. % of the ore is oxidized and consists of three hematitic ore types at slightly higher grades than the primary ore (Renaud et al., 2011).

Figure 11 a) Outcropping layers of iron ore along the crest of the main ridge at Haji-Gak. (Photos by Robert Bohannon, U.S.G.S.), b) Mixed magnetite and semimartite iron ore, c) Euhedral pyrite magnetite ore



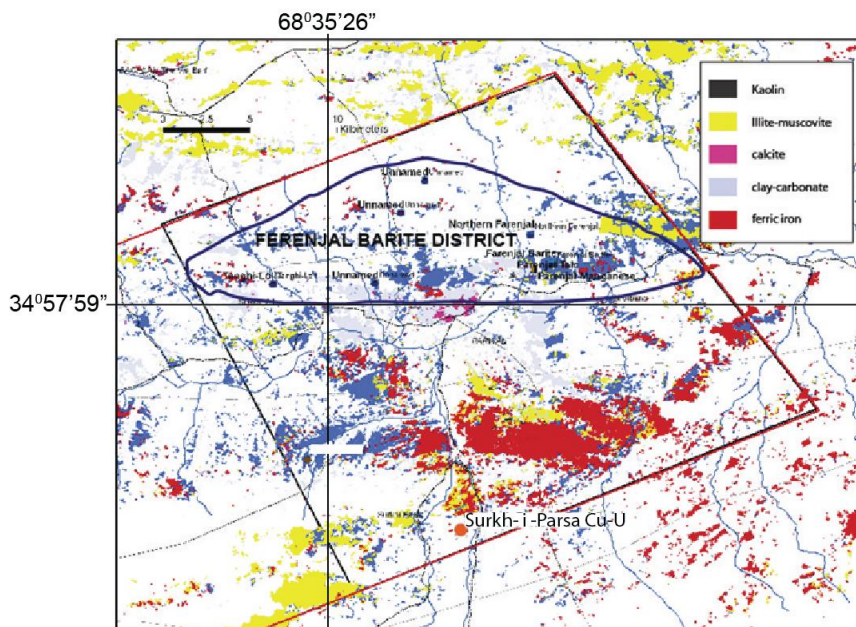
Source: Photos by AGS (2011); from Peters et al. (2007)

The Haji-gak iron deposits have 28.3 million tons with a grade of 62.5% as proven, 396.8 million tons with a grade of 61% Fe as probable, and 1340 million tons as possible and total 1770 million ton iron reserves (Momji & Chaikin, 1960; Mirzad, 1961; Kusov, 1963; Kusov, Smirnov & Reshetnyak, 1965a; Kusov, Smirnov & Reshetnyak, 1965b; Bouladon & de Lapparent, 1975).

NE Haji-Gak Sub Area

It is adjacent to the main Haji-Gak iron deposit and is in its NE. In Chuy, Khaish, Khakriz, Kharzari, Sausang and Zerak iron deposits are observed in metasedimentary rocks. Also include a Barite deposit (Figure 12).

Figure 13 ASTER radiometer image showing the Farenjal subarea, which contains the Farenjal iron and barite district in the north and the Surkh-i-Parso



Source: from Peters et al. (2007), Renaud et al. (2011)

The Darre-i-Neel iron prospect lies 9 km northeast of the Khakriz bed, in the upper part of the Darre-i-Neelee creek. The ore consists of blocky martite formed in skarns and separately exposed ores.

Surkh-o-Parso is located 30 km east of Darre-i-Neel. Blocky fragments of hematite-magnetite ore form the ore deposit; its size and storage conditions are unknown. In addition to iron ores, Pb-Zn-barite ores are also present in this area (Manucharyants, Mirzad & I.K., 1963). Scattered chalcopyrite was found in an area of 9 km² in Carboniferous-Early Permian marbled limestone and quartzite. Uranium minerals have also been found in the formation (Khananov et al., 1967).

The Farenjal barite subfield includes formations in barite deposits and Paleozoic rocks and the Surkh-o-Parso iron-copper-uranium prospect (Shareq et al., 1977). The Farenjal barite and Pb-Zn ore region lies along the Gorbant River basin in an area underlying carbonate-shale and volcanic rocks of Paleozoic age. The area is known for its mineralization of barite, Pb, and Zn. Bottom mineralization is represented by manganese, Fe, Cu, talc and asbestos. Deposits and formations of the Barite and Pb-Zn ore formation are generally found in slip zones in the Lower Carboniferous terrestrial carbonate rocks of the Har-i-Rod Fault. The tops of carbonate barite veins are almost devoid of lead and zinc sulfides.

From a depth of 100 m, calcite-barite ore turns into calcite-sulfide ore, poor in barite and rich in Pb and Zn. Stream sediment sampling revealed halos rich in scheelite, wolframite, and cassiterite, as well as Au and cinnabar. The origin of these minerals is unknown.

Conclusion

Afghanistan has billion tons of high-quality economically exploitable level sedimentary and skarn-type iron deposits. The Haji-Gak iron deposit in Bamyan Province is the best known and largest iron oxide deposit in Afghanistan.

The Haji-Gak Fe deposit is located approximately 100 km W of Kabul in the northeastern part of Afghanistan. The Haji-Gak iron deposits lies in parts of Parwan and Wardak Provinces and some parts of Bamyan, Beshud, Ghorband, Hisa-i-Awal, Markazi, Shekh Ali, Shibar and Surkh-i-Parso Districts. The Haji-Gak Fe area covers an area of 2,079 km² and it is divided into 3 sub-areas; Haji-Gak prospect sub area (180 km²), NE Haji-Gak sub area (381 km²), Farenjal subarea (557 km²).

The area including Haji-Gak iron deposits consist of metavolcanic and metasedimentary rocks of Middle to Late Proterozoic age as well as Paleozoic and Tertiary rocks. the Haji-Gak iron deposit was formed in the Early Paleozoic (probably Silurian to Lower Devonian) based on its stratigraphic position in the Awband Formation, over metamorphosed Proterozoic gneiss and under Late Devonian fossil-bearing formations. The Awband formation hosts most of the iron deposits, which are assumed to be sedimentary exhalative iron-rich fluids that formed lenses on the sea floor during periods of increased volcanic activity. The Haji-Gak iron deposit consists of a series of folded and faulted iron-rich lenses. The lenses are altered and contain cross-cutting iron veins. The iron-bearing rocks are extensively sericitized and silicified.

The Haji-Gak iron deposit surfaces along the S slopes of the mountains as rocky ridges along the NE-SW slope of the ridge crest contains 16 masses of in-situ iron mineralization and 4 masses of fragmented mineralized bulk materials. Mineralized masses are formed as tabular or lenticular masses, the direction and slope of which coincide with the predominant sinuous structure of the region.

In the Haji-Gak subarea, iron ore is primary and oxidized. Up to 100 to 130 m below the existing surface, the mineralized material is partially or completely oxidized. The primary ore (80% of the deposit by volume) contains an average of 61.3% iron by weight consists mainly magnetite (40–90%) and pyrite (2–35%) as primary minerals, minor amount hematite, martite, chalcopyrite and other sulfides as well as carbonate and silicate minerals and barite as gangue minerals. The primary ores are dense, fractured, steel-black in color and exhibit massive, massive-banded, and mottled textures with fine to medium and rare coarse-grained, xenomorphic, and idiomorphic grains.

Primary semioxidized ore represented by hydrogoethite-semimartite, hydrogoethite-hematite-semimartite, and carbonate-semimartite ores.

The remaining 20 vol. % of the ore is oxidized and consists of three hematitic ore types at slightly higher grades than the primary ore.

The Haji-gak iron deposits have 28.3 million tons with a grade of 62.5% as proven, 396.8 million tons with a grade of 61% Fe as probable, and 1340 million tons as possible and total 1770 million ton iron reserves.

NE Haji-Gak Sub Area is adjacent to the main Haji-Gak iron deposit and is in its NE have total iron reserves are 300 Mt. In Chuy, Khaish, Khakriz, Kharzari, Sausang and Zerak iron deposits are observed in metasedimentary rocks. Also include a Barite deposit.

Farenjal Sub Area in the NE section of the Haji-Gak iron deposits, the Paleozoic strata include Farenjal Fe, barite, manganese, Pb-Zn, and U ore regions. In addition, Cu, asbestos and talc mineralizations are monitored.

Afghanistan's long-term economic growth, it is crucial that underground resources be explored in more detail using comprehensive scientific methods, the general characteristics of mineral deposits be revealed, and their exploitation and integrating into the economy are crucial.

References

Abdullah, S. H., & Chmyriov, V. M. (1977). *Geologiya i poleznye iskopaemye Afganistana. Kniga 1. Nedra, Geologiy, Moscow, 535 pp.*

AGS. (1967). *Geological structure of the Haji-Gak iron deposit and its commercial value*. Afghanistan Geological and Mineral Survey; Kabul, 13 pp.

AGS. (2011). Kabul: Mineral resources of Afghanistan (2nd ed.) Geological Survey of Afghanistan, Ministry and Mining Presidency of Afghanistan.

Bekker, A., Slack, J., Planavsky, N., Krapez, B., Hofman, A., Konhauser, K., & Rouxel, O. (2010). Iron formation—The sedimentary products of a complex interplay among mantle, tectonic, oceanic, and biospheric processes: *Economic Geology*, 105, 467–508.

Bouladon, J., & de Lapparent, A. (1975). Le minerais de fer d'Hajigak (Afghanistan); position stratigraphique, cadre géologique et type du gisement [The iron minerals of the Haji-Gak Pass, Afghanistan; stratigraphic position, geological evolution and type of deposit]: *Mineralium Deposita*, 10 (1), 13–25.

Brueckl, K. (1935). *Über die geologie von Badakhshan und Kataghan (Afghanistan)* [The geology of Badakhshan and Kataghan (Afghanistan)]. *Neues Jahrbuch für Mineralogie, Geologie und Paläontologie*, 74, (B-3), 360–401.

Brueckl, K. (1936). *Die minerallagerstätten von Ostafghanistan; versuch einer gliederung nach genetischen gesichtspunkten* [The mineral regions of east Afghanistan; their origins and characteristics]. *Neues Jahrbuch für Mineralogie, Geologie und Paläontologie, Abhandlungen*, pt. A, Mineralogie, Petrographie, 1, 1–97.

Bybochkin, A., & Kurotchenko, V. (1960). *Report on preliminary geological-economic evaluation of minerals of Afghanistan and recommendation on orientation of geological-reconnaissance works for the second five-year plan: Kabul, Afghanistan.*

Cannon, W. (1986a). Descriptive model of Algoma Fe. *Mineral deposit models (Eds: D.P. Cox and D.A. Singer); U.S. Geological Survey Bulletin 1693, 198 pp.*

Cannon, W. (1986b). Descriptive model of Superior Fe,. *Mineral deposit models (Eds: D.P. Cox and D.A. Singer); U.S. Geological Survey Bulletin 1693, 228 pp.*

Cox, D. (1986). Descriptive model of Olympic Dam Cu-Au-U. *Mineral deposit models (Eds: D.P. Cox and D.A. Singer), U.S. Geological Survey Bulletin 1693, 200 pp.*

Doebrich, J., Wahl, R., Ludington, S., Chirico, P., Wandrey, C., Bohannon, R., . . . Bliss, J. (2006). Geologic and mineral resource map of Afghanistan:. *U.S. Geological Survey Open File Report 2006-1038, scale 1:850,000;.*

Dronov, V., K. S., Sborshchikov, I., Svezhentsov, V., Chistyakov, A., Zelensky, E., & Cherepov, P. (1972). The geology and minerals of North Afghanistan . *(parts of map sheets 400-II and 500-I, the Kaysar-Hari Rod Interfluve area): Kabul, DGMS, 44.*

ESCAP. (1995). *Geology and mineral resources of Afghanistan.* United Nations, Atlas of Mineral Resources of the Economic and Social Commission for Asia and the Pacific Region (ESCAP), New York, 12, 85 pp.

Haynes, D. (2000). Iron oxide copper gold deposits-Their position in the ore deposit spectrum and modes of origin; Hydrothermal iron oxide copper-gold and related deposits—A

global perspective (Ed: T.M. Porter): Adelaide, Australian Mineral Foundation, 71–90.

Hitzman, M. (2000). Iron oxide-Cu-Au deposits—Where, when, and why; Hydrothermal iron oxide copper-gold and related deposits—A global perspective (Ed: T.M. Porter) : Adelaide, Australian Mineral Foundation, 9–25.

Kansun, G., & Afzali, A. (2022). Geology, Petrographic Characteristics and Tectonic Structure of Paleoproterozoic basement of Kabul Block (North Eastern Afghanistan), Initial Findings. *International Journal of Multidisciplinary Studies and Innovative Technologies (IJMSIT)*, 6 (1), 117-133.

Karapetov, S., Stazhilo-Alekseyev, K., & Kotchetkov, A. (1970). The geology and minerals of the eastern part of central Afghanistan: Kabul, Afghanistan, Afghanistan Geological and Mineral Survey.

Khananov, R., Plotnikov, G., Bayazitov, R., Sayapin, V., & Trifonov, A. (1967). *Report on revised estimation investigations of mineral deposits and occurrences of copper, lead, zinc and gold in 1965—V. I–II*. Kabul, Afghanistan, Afghanistan Geological and Mineral Survey.

Kusov, I. (1963). Geological mapping, prospecting, and exploration on the iron deposit of Hajigak: Kabul, Afghanistan, . *Afghanistan Geological and Mineral Survey USSR v/o Technoexport contract 640, 88 pp*.

Kusov, I., Smirnov, M., & Reshetnyak, V. (1965a). Report on prospecting and survey at iron occurrences in central Afghanistan and the Hajigak iron deposit's estimated reserves. *Afghanistan Geological and Mineral Survey*.

Kusov, I., Smirnov, M., & Reshetnyak, V. (1965b). Report on the results of geological prospecting, survey and exploration of iron

deposits and occurrences in central Afghanistan with the data on iron ore reserves estimation of the Haji-Gak deposit carried out in 1963–1964. *Kabul, Afghanistan, Afghanistan Geological and Mineral Survey USSR v/o Technoexport contract no. 640, 3 v.*

Livo, K. E., & Giles, S. A. (2011). Analysis of Imaging Spectrometer Data for the Haji-Gak Area of Interest. *Summaries of Important Areas for Mineral Investment and Production Opportunities of Nonfuel Minerals in Afghanistan, Chapter 7B. (Eds: Stephen G. Peters, Trude V.V. King, Thomas J. Mack, Michael P. Chornack, I, 7B, 499-548.*

Manucharyants, O., Mirzad, S., & I.K., K. (1963). *Project of geological survey, prospecting, and exploration works on iron ores of the Hajigak deposit: Kabul, Afghanistan, . Afghanistan Geological and Mineral Survey.*

Mirzad, S. (1961). *Iron ore deposit of the Hajigak pass: Jundun, no. 26, appendix.*

Momji, G., & Chaikin, S. (1960). *Iron ores of Afghanistan. Kabul, Afghanistan, Afghanistan Geological and Mineral Survey.*

Nishiwaki, C. (1970). Iron ore deposits of the Middle East, Asia and the Far East;. *Survey of world iron ore resources—Occurrence, appraisal and use: United Nations Committee of Experts on Iron Ore Resources, 102-106. içinde*

Orris, G. J., & Bliss, J. D. (2002). Mines and Mineral Occurrences of Afghanistan. *United States Geological Survey, Open-File Report 02-110, Tucson, Arizona, 95 pp.*

Peters, S. G. (2007). *Preliminary Assessment of Non-Fuel Mineral Resources of Afghanistan;. USGS Minerals Fact Sheet 2007-3063.*

Peters, S. G., Ludington, S., Orris, G. J., Sutphin, D. M., Bliss, J. D., & Rytuba, J. J. (2007). *Preliminary Non-Fuel Mineral Resource Assessment of Afghanistan*. Geological Survey (US), No: 2007-1214, 045-178.

Renaud, K., Sutphin, D. M., Peters, S., & Drew, L. (2011). Summary of the Haji-Gak Iron Area of Interest;. *Summaries of Important Areas for Mineral Investment and Production Opportunities of Nonfuel Minerals in Afghanistan, Chapter 7B*. (Eds: Stephen G. Peters, Trude V.V. King, Thomas J. Mack, Michael P. Chornack), 7A, 450-498;.

Shareq, A., Chmyriov, V. M., Stazhilo-Alekseev, K. F., Dronov, V. I., Gannan, P. J., Rossovskiy, L. N., . . . Malyarov, E. P. (1977). Mineral resources of Afghanistan (2nd edition); Kabul, Afghanistan, Afghanistan Geological and Mineral Survey, 419 p. .

Shroder, J., Cookson, F., Belasky, P., Roshan, Y., Watrel, R., Nathan, R., & Lerner, H. (1992). *Mineral Resources in Afghanistan*. Nathan Berger Aghanstan Studies Project, Final Report. AID, Representative for Afghan Affirs, 87 pp.

Sutphin, D., Renaud, K., & Drew, L. (2011). A Reevaluation of the Mineral Resources of the Haji-Gak Iron Deposit. *Summaries of Important Areas for Mineral Investment and Production Opportunities of Nonfuel Minerals in Afghanistan, Chapter 7D*. (Eds: Stephen G. Peters, Trude V.V. King, Thomas J. Mack, Michael P. Chornack), I, 7D, 570-597.

COPPER DEPOSITS IN AFGHANISTAN AND THE BALKHAB COPPER DEPOSIT

**GÜRSEL KANSUN⁴
ALPER DÜLGER⁵
FETULLAH ARIK⁶**

Introduction

Tectonic Structure of Afghanistan

Afghanistan lies within the Alpine–Himalayan belt, which developed as a result of the Late Paleogene collision between the Indian and Arabian plates and the Eurasian plate (Boulin, 1990) (Figure 1).

Afghanistan consists of a complex assemblage of terranes, most of which originated from Gondwana, that were accreted to the southern margin of Eurasia before and during the India–Eurasia plate collision (Şengör, 1984; Boulin, 1991). These areas consist of the

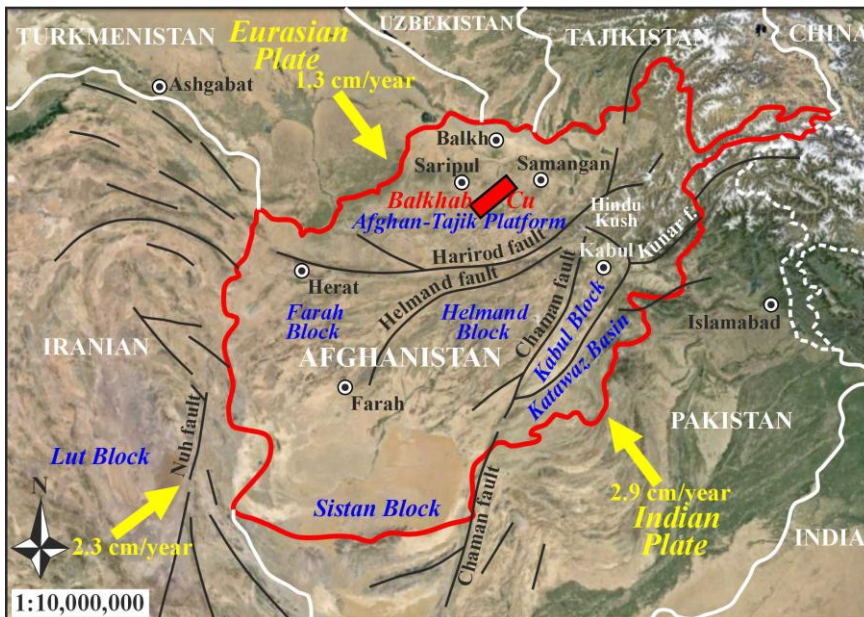
⁴Assistant Professor, Konya Technical University, Geological Engineering, 0000-0002-4581-6076

⁵ Research Assistant, Konya Technical University, Geological Engineering, 0000-0003-3380-7663

⁶ Professor, Konya Technical University, Geological Engineering, 0000-0003-0833-7778

Afghan–Tajik Platform to the north (Brookfield & Hashmat, 2001), the Katawaz Basin to the southeast (Treloar & Izatt, 1993), and the Afghan Central Blocks located between them (Figures 1 and 2).

Figure 1 The position and tectonic activities of Afghanistan within the Alpine–Himalayan orogenic belt. The arrows indicate the relative plate motions and velocities between the Indian, Eurasian, and Arabian plates

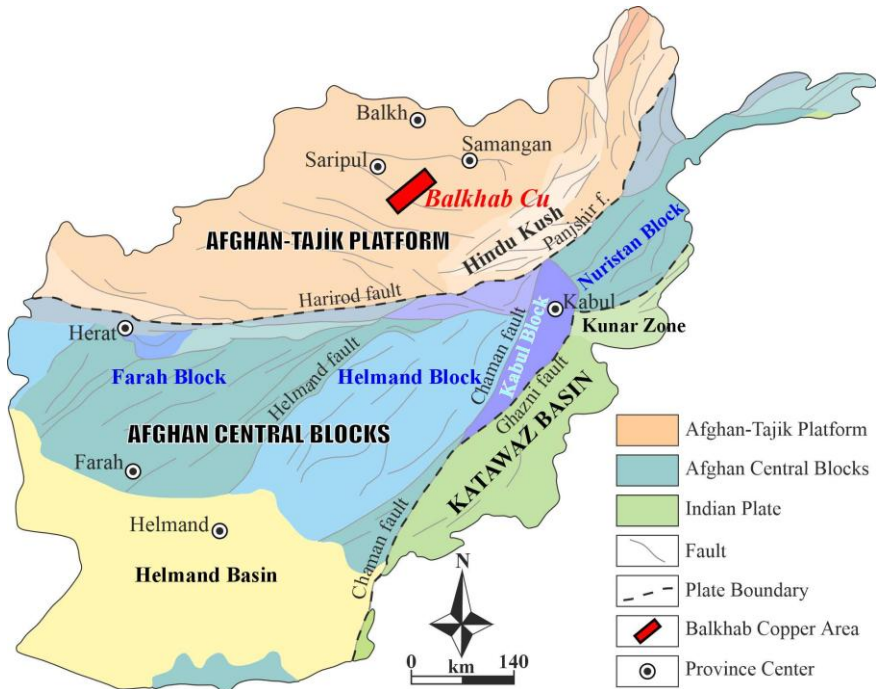


Source: Revised from Ambraseys & Bilham (2003), Crone (2007), Afzali (2024), Kansun & Afzali (2022)

The Afghan Central Blocks are divided into three blocks: the Helmand Block, the Farah Block, and the Kabul Block, whose location is disputed. The Kabul Block is defined as the easternmost part of the Afghan Central Blocks according to Andritzky (1967). In contrast, Tapponnier et al. (1981) and Treloar & Izatt (1993) propose that the Kabul Block is a separate terrane that was accreted to the Afghan Central Blocks prior to the collision between the Eurasian and Indian plates. The Katawaz Basin represents the northwestern

continental margin of the Indian Plate. The Afghan Central Blocks, the Kabul Block, and the Nuristan Block mark the Eurasia–India boundary (Collet, Faryad & Mosazai, 2015).

Figure 2 Tectonic outlines of Afghanistan



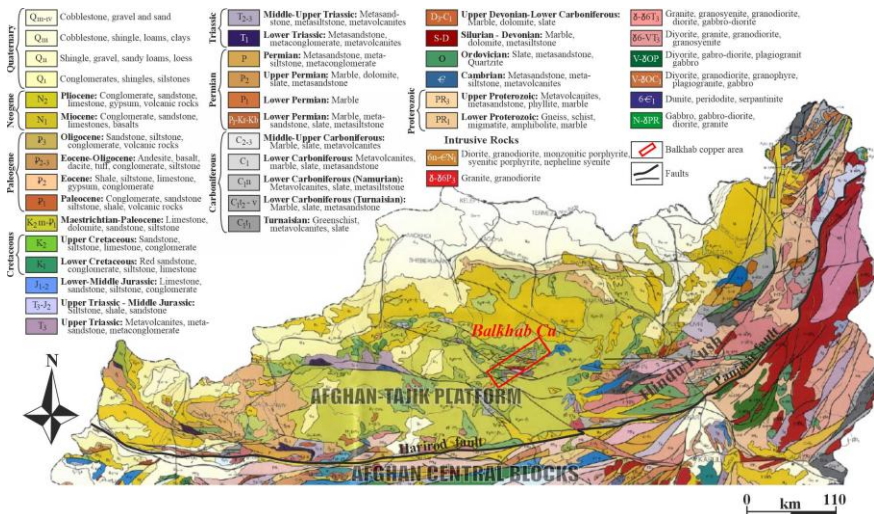
Source: Revised from Boulin (1991), Leven (1997), Bohannon (2010), Collet Faryad & Mosazai (2015)

Afghan-Tajik Platform

The Afghan-Tajik Platform, representing the Eurasian plate, forms the Parapamissus and western Hindukush mountains in northern Afghanistan and the high plains of the Amu Darya basin (Figure 2). This platform contains pre-Jurassic basement rocks at the base. The basement rocks consist of Proterozoic and Cambrian marine sediments developed on oceanic crust, an Ordovician–Early Devonian passive-margin sequence, an Upper Devonian–Lower Carboniferous magmatic arc sequence, a Lower Carboniferous–

Permian rift–passive-margin sequence, and a Triassic continental magmatic arc succession (Figure 3) (Brookfield & Hashmat, 2001; ESCAP, 1995).

Figure 3 Geological map of the Afghan-Tajik Platform



Source: Revised from (ESCAP, 1995)

These basement rocks are overlain by Mesozoic-Paleogene cover rocks and Neogene continental clastics (Figure 3).

The Mesozoic-Paleogene consists of four units: 1) Late Triassic-Middle Jurassic rift sequence where clastic rocks such as siltstone, shale and sandstone are common. 2) Middle-Upper Jurassic sequence. It consists of clastic and carbonate rocks, from continental and marine Bathonian to Lower Kimmeridgian. Evaporite-bearing clastic rocks of Upper Kimmeridgian-Tithonian age are observed overlying these. 3) The Cretaceous sequence rests unconformably on older units. It consists of Lower Cretaceous evaporite-bearing and red-colored conglomerate, sandstone, siltstone, and limestone. It is overlain unconformably by Cenomanian–Maastrichtian shallow-marine limestones and clastics. 4) Paleogene sequence. The Paleocene and Eocene consist of

conglomerate, sandstone, siltstone, and shale, locally containing volcanic rocks. The succession from the Late Eocene to the Oligocene comprises widespread andesite, basalt, dacite, and tuffs at the base, overlain by clastic units that include levels of volcanic rocks (Brookfield & Hashmat, 2001; ESCAP, 1995).

The Neogene sequence consists of continental sediments of variable thickness. This sequence is composed of conglomerate, sandstone, siltstone, and limestone that contain levels of Miocene–Pliocene acidic to basic volcanic rocks and gypsum.

Copper Deposits in Afghanistan

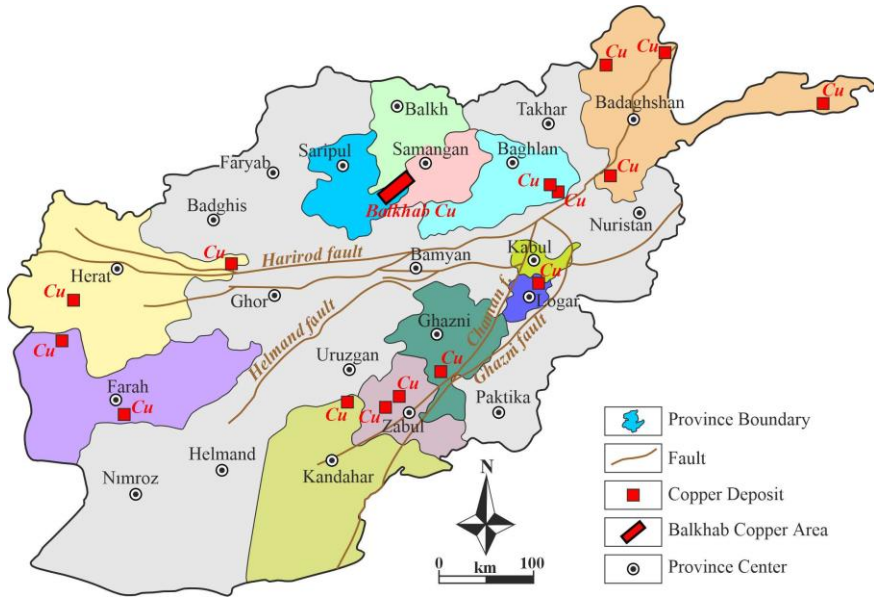
Afghanistan contains significant amounts of copper, as well as base metals such as bismuth, lead, zinc, and tungsten; ferrous and ferroalloy metals such as chromium and molybdenum; light metals including aluminum, beryllium, and lithium; precious metals such as gold and silver; radioactive elements including uranium and thorium; rare metals such as tantalum and rubidium; and rare earth elements. Additionally, significant deposits of oil, coal, barite, fluorite, rock salt, and sulfide are observed. There are around 300 identified copper deposits, occurrences, and indications in Afghanistan. Various copper mineralizations occur in rocks ranging in age from the Proterozoic to the Neogene (ESCAP, 1995; Afghanistan Copper Mines, 2017).

Important copper occurrences in Afghanistan occur particularly in Logar, Saripul-Balkh-Samangan, Ghazni, Baghlan, Badaghshan, Herat, Farah, Kandahar, Kabul and Zabul provinces (Figure 4). The most important copper formations are located in Aynak, Balkhab, Duser-Shaida-Misgaran and Zarkashan (Jilani, Ahmad & Zuhail, 2024; ESCAP, 1995; Abdullah et al., 1977).

Aynak copper deposit, one of the largest copper deposits in the world, is located in Logar Province, 40 km southeast of Kabul

(Figure 4) and is the largest known copper deposit in Afghanistan. Here, copper occurrences are observed in dolomitic marble, quartz schist and quartz-biotite-calcschist in the Vendian (Upper Proterozoic) – Cambrian aged Loy Khawar formation. Aynak mine is a stratiform type copper deposit and has reserves of 690 million metric tons of ore containing 1.65% copper.

Figure 4 Important copper deposits in Afghanistan



Source: The study made use of (ESCAP, 1995) data for the copper areas

The Balkhab copper deposit, which is the subject of this study, is located within the boundaries of the Balkhab district of Saripul Province, the Kishindih district of Balkh Province, and the Dara-i-Suf district of Samangan Province in northern Afghanistan (Figure 4). The Balkhab copper volcanogenic massive sulphide deposit is associated with pre-Triassic, particularly Ordovician, rocks (Peters et al., 2007). The copper mineralization consists of a 4,000-5,000 m long, 300-400 m wide deformed and faulted rock containing silicified limonite (Peters et al., 2011), and this rock

contains 1.66% pure copper. Estimated reserves exceed 150 million tons.

The Duser-Shaida-Misgaran copper deposit is located in the Adraskan region of Herat Province (Figure 4). The Duser subarea is known for its copper, zinc and rare gold concentrations in siliceous limonitic rocks associated with metamorphic volcanic rocks and is a volcanogenic massive sulphide deposit. Mineralization in the Duser subfield is likely associated with a continental back-arc environment. The porphyry copper deposit in the Shaida subarea contains copper and zinc as massive veins and disseminated ores within altered volcanic layers cut by Oligocene granitoids. Here, the copper mineralization zone coincides with a 200-300 m wide, strongly fractured, limonitized and kaolinitized fault zone. This mineralization zone is 2.6 km long and 300 to 500 m wide, and contains 0.27-3.02 wt% copper and 0.02-0.37 wt% zinc. The Misgaran subarea is notable for its abundant tin and lead-rich skarn and polymetallic veins and has been interpreted as a tin skarn deposit. It is estimated that there are 4.8 million metric tons (Mt) of ore containing 1.1% copper and 1.2% zinc by weight in the Shaida sub-area (Tucker, Schulz & Peters, 2011).

The Zarkashan copper-gold area is located in the south of Ghazni Province (Figure 4). Late Proterozoic metamorphic rocks, Lower Paleozoic dolomite, limestone, shale and Carboniferous - Early Permian mafic volcanic rocks, sandstone, shale, siltstone are observed in the region. These rocks were cut by the Zarkashan intrusive bodies, which consists of adamellite, diorite, gabbro and granodioritic stocks and plutons during the Late Cretaceous - Paleocene period. It has been determined that there is 0.44-1.7% copper in the region (Peters et al., 2011).

Balkhab Copper Area

Location of the Balkhab Copper Field and Previous Studies

The Balkhab copper area is located in northern Afghanistan, within the boundaries of Balkhab district of Saripul Province, Kishindih district of Balkh Province, and Dara-i-Suf district of Samangan Province (Figure 5). It is approximately 150 kilometers southeast of Saripul and approximately 130 kilometers northwest of Bamyan. The main Balkhab copper area covers 1,858 km² and the Balkhab copper subfield covers 321 km² (Figure 5). The topography of the Balkhab copper area is characterized by a steep-sided valley containing the Balkh River, which flows from southwest to northeast. The base of this valley is between 950 and 1,400 m above sea level. Elevations on the sides of the valley reach up to 4,028 m.

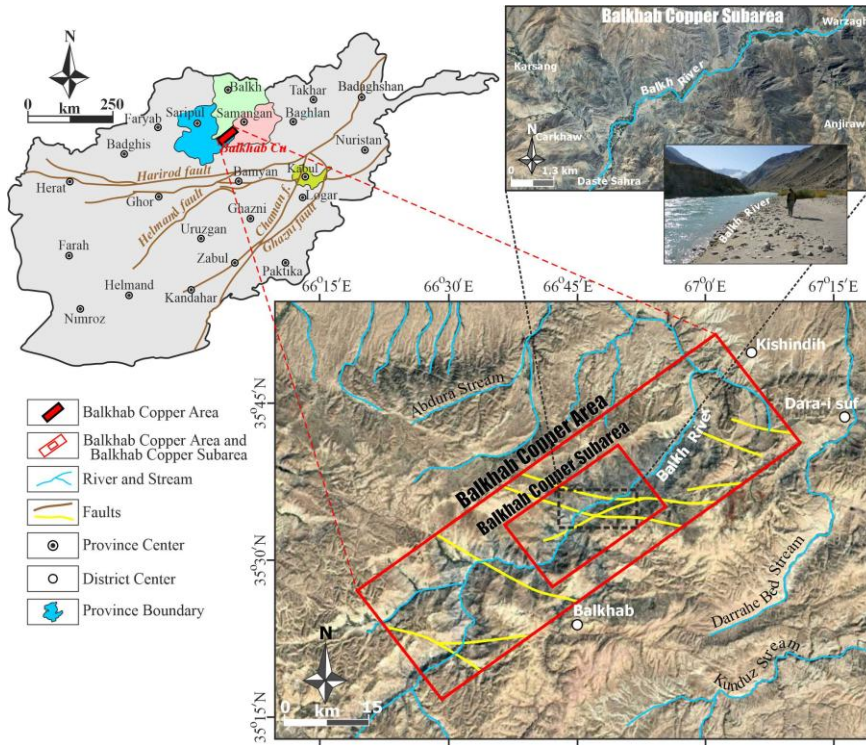
Mining activities at the Balkhab copper deposit date back 3,000 years. In the region, Kafarskiy et al. (1972) produced the geological map of the Balkhab copper exploration area and carried out trench and grid sampling in the copper zones. Sborshchikov et al. (1973) have revealed the regional geology of northern Afghanistan.

The Balkhab copper deposit was studied by Soviet geologists in 1972, 1973, and 1977, and the geological sketch of the area was produced. Abdullah et al. (1977), the Economic and Social Commission for Asia and the Pacific (ESCAP, 1995) and the Japan Metal Mining Agency (MMAJ, 1998) studied mineral formations in Afghanistan and provided information about the Balkhab copper deposit.

Orris & Bliss (2002) and Doebrich et al. (2006) state that the Balkhab copper area contains rather large copper deposits and that these are hydrothermal–metasomatic in origin and represent a volcanogenic massive sulfide deposit. Peters et al. (2007) said that

this deposit was either a Kuroko subtype or a bimodal-felsic type volcanic massive sulfide deposit. In 2009, Engineer Abdul Gaffer and his team from the Geological Survey of Afghanistan conducted geological mapping in the region and stated that the copper mineralization zone was more than 60 m thick.

Figure 5 Location of the Balkhab copper area and Balkhab copper subarea in northern Afghanistan



Source: The study made use of (Mack & Chornack, 2011) for the locations of the Balkhab copper area and the Balkhab copper subarea and made use of (Hoefen & Johnson, 2011) for the faults in the Balkhab copper area and the Balkhab copper subarea

Sabins & Ellis (2010a) and Sabins & Ellis (2010b) conducted remote sensing targeting analyses for copper deposits and coal formations in the Balkhab copper area. Peters et al., (2011) state that

in the Balkhab copper area, the copper mineralization consists of a deformed and faulted rock containing silicified limonite, measuring 4,000 to 5,000 m in length and 300 to 400 m in width, and that this rock contains between 0.25 and 1.34 wt% copper. These researchers stated that abundant malachite, azurite, pyrite, and scattered chalcopyrite, bornite, and galena were observed in the area.

Hoefen & Johnson (2011) analyzed the hyperspectral remote sensing data collected over the Balkhab copper area using spectroscopic methods to determine the occurrence of selected surface materials. These researchers stated that the region has potential for volcanogenic massive sulfide, coal, and possible gold deposits, and that muscovite, kaolinite, chlorite or epidote, and montmorillonite exhibit distinct patterns in the area. They also identified small but distinct formations of jarosite, hydrated silica, and pyrophyllite in the area, which may be associated with hydrothermal alteration.

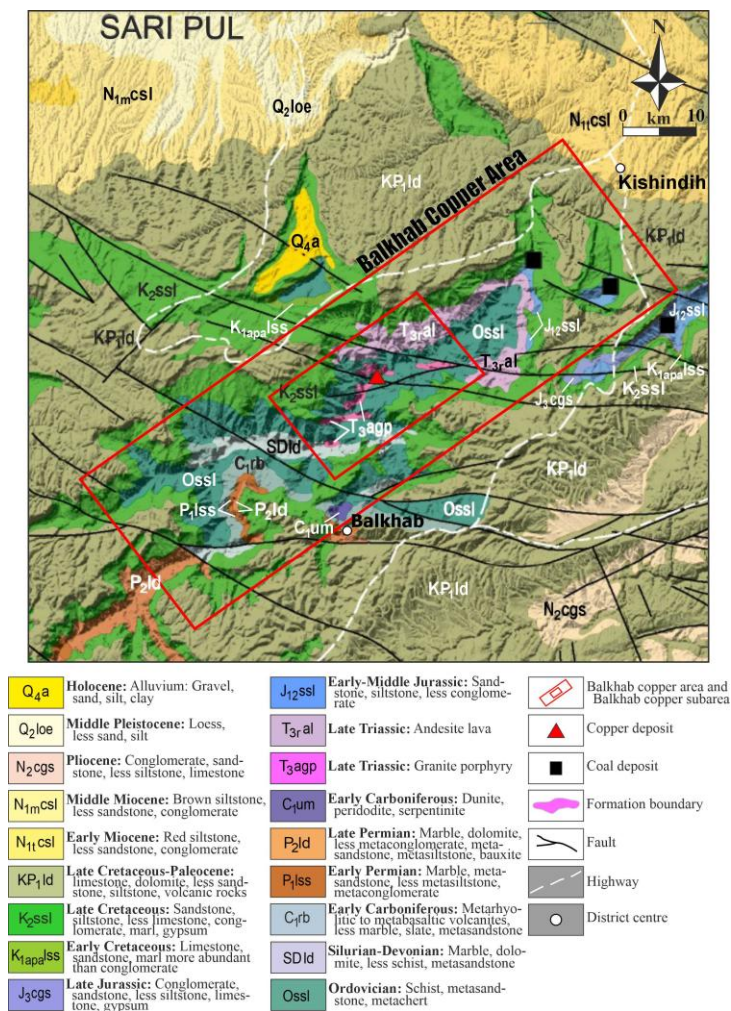
Jilani, Ahmad & Zuhail (2024) state that the main minerals constituting the copper ore in the Mir Sayed Murad area of Balkhab district are feldspar, quartz, copper, amphibole, plagioclase, pyroxene, calcite, sulfur and iron oxide, and trace amounts of pyrite and biotite are also present. They said that these minerals are mainly associated with rhyolite, basalt and andesitic rocks, and that sedimentary rocks such as sandstone, pyrite clay and silicic clay also contain copper minerals. They indicate that, in addition to copper, the copper ore contains varying amounts of other elements such as silicon, sulfur, iron, and aluminum.

Stratigraphy of the Balkhab Copper Area

Paleozoic and Mesozoic lithologies crop out in the Balkhab copper area (Figure 6).

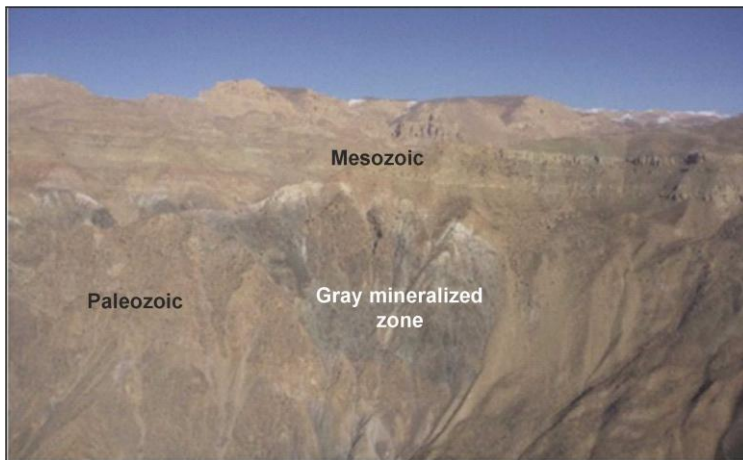
In the Balkhab copper area, Paleozoic metaclastic rocks, metacarbonates, and metavolcanites are unconformably overlain by nearly horizontal Mesozoic metaclastic rocks and metacarbonates (Figure 7), and are cut by Mesozoic metaplutonic rocks and metavolcanites.

Figure 6 Geological map of the Balkhab copper area and its immediate surroundings



Source: From (Doebrich et al., 2006)

Figure 7 Paleozoic lithologies in the Balkhab copper area, overlain by nearly horizontal Mesozoic lithologies, and the gray-colored mineralized zone

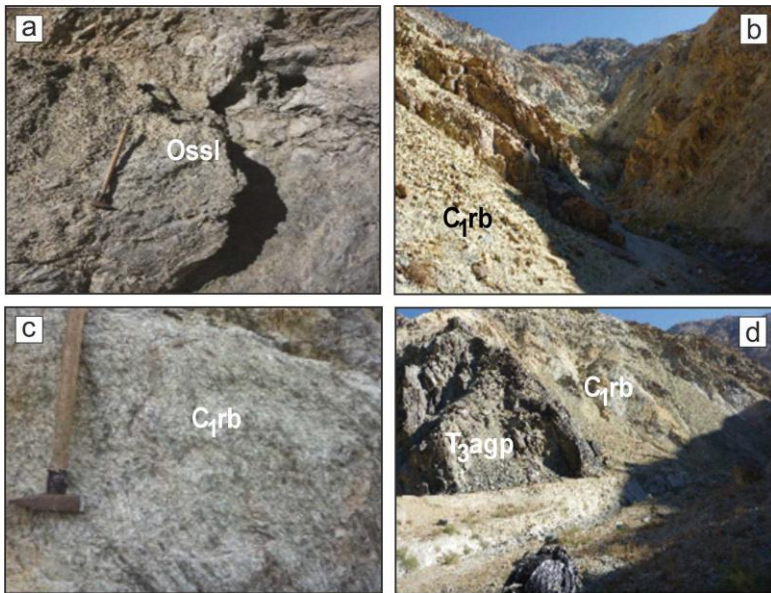


Source: The photograph used in this study were sourced from Peters et al. (2011), The Photograph by Robert D. Tucker, U.S. Geological Survey

In the region, there are Ordovician aged schist, phyllite, metasandstone, metasiltstone and metachert (Ossl) showing low-grade metamorphism features at the bottom (Figures 6, 8a and 9b). Upsection, Silurian–Devonian marble and dolomite are observed, along with occasional schist, phyllite, and metasandstone (SDld). These lithologies are covered by Early Carboniferous (Missippian) aged metavolcanites and metasedimentary rocks (C₁rb) (Figures 8b and c). Meta volcanites consist of rocks with compositions ranging from metariolite to metabasalt. Metasediments that are less widespread are composed of marble, slate, metasandstone and metaconglomerate. Overlying these units unconformably are Early Permian lithologies composed of crystallized limestone and metasandstone, and locally metaconglomerate and metasiltstone (P₁lss). Towards the top, Late Permian lithologies (P₂ld) are observed, consisting predominantly of crystallized limestone and

dolomite, and locally of metaconglomerate, metasandstone, metasiltstone, and phyllite (Figure 6).

Figure 8 Lithologies observed in the south of the Balkh River in the Balkhab copper subarea. a) Low-grade metapelitic rocks of Ordovician age (Ossl) (66,73318° E – 35,55659° N), b and c) Early Carboniferous metarhyolites showing schistosity (C_{1rb}), (b: 66,73750° E – 35,55285° N, c: 66,73747° E – 35,55294° N), d) Dark-colored, highly sheared Late Triassic granite porphyry faulted against steeply dipping Early Carboniferous metarhyolites (C_{1rb})



Source: The photographs and the coordinates used in this study were sourced from Peters et al. (2011), The photographs by Robert D. Tucker, U.S. Geological Survey

These basement rocks are covered with a tectonic contact by Early Carboniferous dunite, peridotite and serpentinite (C_{1um}) to the south of the Balkh River. To the north of the Balkh River, these basement rocks are cut by Late Triassic aged, medium-fine grained granite porphyries (T_{3agp}) (Figures 6 and 8d).

In the eastern part of the Balkhab copper area, Late Triassic andesitic lavas (T_{3ral}) overlie Ordovician lithologies (Figure 6). Unconformably overlying these lavas are Early–Middle Jurassic lithologies, consisting predominantly of sandstone and siltstone, and locally of conglomerate (J_{12ssl}). In this area, upsection, Late Jurassic lithologies (J_{3cgs}), consisting predominantly of conglomerate and sandstone and locally of siltstone, limestone, and gypsum, are observed, along with Early Cretaceous lithologies ($K_{1apa1ss}$), which consist mainly of limestone, sandstone, marl, and locally conglomerate (Figure 6).

Late Cretaceous lithologies (K_{2ssl}) are observed throughout the Balkhab copper field (Figure 6). In the region, the Late Cretaceous is composed of largely sandstone and siltstone and occasionally limestone, conglomerate, marl and gypsum. Late Cretaceous–Paleocene lithologies (KP_{1ld}), consisting of limestone, marl and dolomite and occasionally sandstone, siltstone, gypsum, conglomerate and volcanic rocks, are observed on this unit. In the Balkhab copper field, Early Miocene aged red siltstone, sandstone and conglomerate (N_{1tcsl}) are located at the top.

Coal occurrences are observed in two separate areas in the northeastern part of the Balkhab copper area. The base of the coal sequences lies within Late Cretaceous lithologies, while the upper part of the sequences is mostly traced near the base of the Late Cretaceous–Paleocene lithologies. These locations indicate that the age of coal formations in the Balkhab copper area is Late Cretaceous. In contrast, ESCAP (1995) states that the Shabashak, Darwaza, Dahane-tor, Sar-e Asia, and Lela coal deposits located near Dara-i Suf District in Samangan Province occur within Lower–Middle Jurassic formations, and therefore these coal deposits are of Lower–Middle Jurassic age.

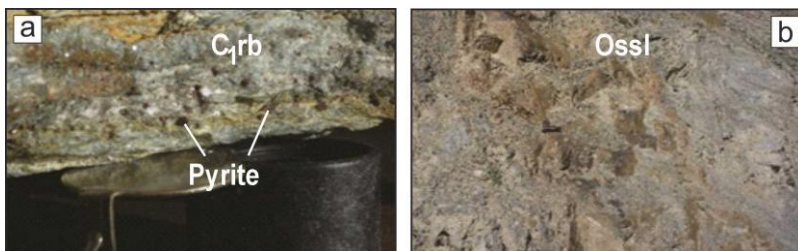
In the Balkhab copper area, Ordovician and Silurian-Devonian aged metapelitic, metapsammitic and metacarbonate rocks were intensely folded as a result of deformations and gained fractured structures such as faults and cracks. These metapelitic rocks consist of low-grade phyllites, schists and metasiltstones. Chlorite, muscovite and sericite are common in phyllites and schists. Peters et al. (2011) stated that within the chlorite-rich Ordovician and Silurian-Devonian phyllites and schists, layers and lenses of black chert and jasper (Figure 9b), blocks of serpentinite, and extensive sheet-like layers of brecciated and altered quartzofeldspathic schistose felsic volcanic rocks are observed. In contrast, the quartzofeldspathic felsic volcanic rocks within the phyllites and schists should probably be Early Carboniferous metariolites showing schistosity (Figures 8b, c and d).

Peters et al. (2011) stated that in the Balkhab copper field, copper-sulfide mineralized zones are located in or near quartzofeldspathic rocks (felsic volcanic rocks). Additionally, these researchers said that most of the quartzofeldspathic rocks are densely mineralized with pyrite, chalcopyrite, and bornite as porphyroblastic euhedral cubes in centimeter-to-meter-thick zones (Figure 9a). This mineralization must have developed as a result of Early Carboniferous metarhyolites cutting the Ordovician and Silurian-Devonian metapelitic-metapsammitic rocks in the area and, simultaneously and/or subsequently, the emplacement of hot hydrothermal solutions associated with the metarhyolites into both the metapelitic rocks and the metarhyolites (Figure 9a) along foliation and fracture zones.

Late Triassic granite porphyries are observed at lower elevations of the Balkh River valley in the Balkhab copper subarea (Figures 6 and 8d). Granite porphyries are typical with their fine-medium grains and phenocrystalline porphyritic textures. According to Peters et al. (2011), trace amounts of valuable base metals are seen

in these rocks, which show propylitic alteration and contain quartz-pyrite veins that are continuous throughout.

Figure 9 In Balkhab copper area, a) Euhedral cubic pyrites in Early Carboniferous metarhyolite (C_{1rb}), b) Brown weathered black metachert and metasiltstone lens within Ordovician aged chlorite schist (Ossl)



Source: The photographs used in this study were sourced from (Peters, Tucker, Gaffer, & Hubbard, 2011), The photographs by Robert D. Tucker, U.S. Geological Survey

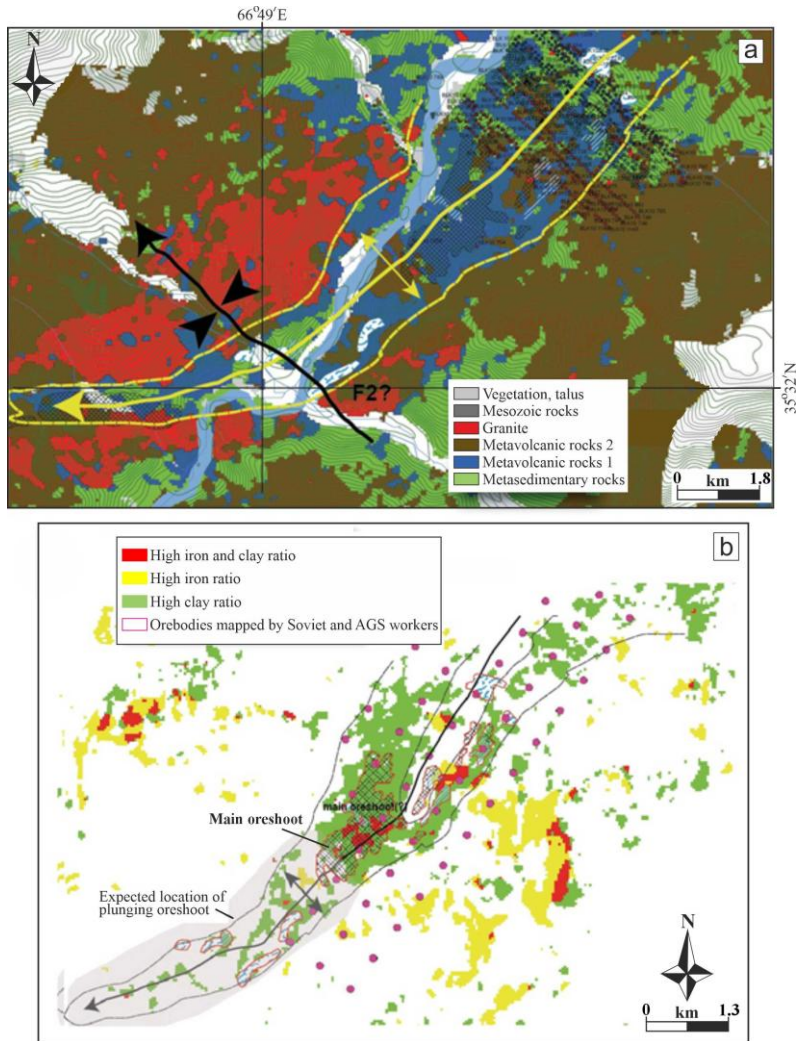
The host rocks surrounding the copper mineralization in the Balkhab copper area are foliated toward the east and contain shear zones. Fold structures and faults are very intense in these host rocks. Shear zones lie parallel to the foliation and show mylonitic features. In this area, on the high slopes of the Balkh River valley, the copper mineralization closest to the Mesozoic contact is the most oxidized, whereas the mineralized zones on the lower slopes well below the Mesozoic contact must lie beneath the original paleo-oxidation zone (Peters et al., 2011).

Characteristics and Metallogenesis of Balkhab Copper Deposit

Kafarskiy et al. (1972) identified a tectonic zone containing Ordovician(?) aged sandy schist beneath Mesozoic (Upper Triassic) lithologies in the Balkhab copper deposit. According to Kafarskiy et al. (1972) and Abdullah et al. (1977), the Balkhab copper deposit is a mineralized rock of copper and lead in a zone containing a maximum copper concentration of 1.66% by weight. Sabins & Ellis

(2010a) have created a geological map of the main mineralized zone of the Balkhab copper area using ASTER imagery (Figure 10).

Figure 10 Structural geology of the mineralized zone in the Balkhab main copper area. a) Geological map, b) Hyperspectral anomalies shown together with ‘envelope’ of fold interpreted from the geological map



Source: (Kafarskiy et al., 1972) and (Sabins & Ellis, 2010a)

This map interprets the ore zones mapped by Kafarskiy et al. (1972) as being located within the deformation sheath of folded metavolcanic stratigraphy. This mineralized zone appears as a grey rock layer (Figure 7) with tones imparted by sulfide minerals along the slope (Peters et al., 2011).

Sabins & Ellis (2010a), in the Balkhab copper area, identified an “envelope” (Figure 10) surrounding the mapped mineralized masses and metavolcanic rocks, marking a southwestward-dipping isoclinal fold, and also including iron and clay alteration zones (Peters et al., 2011). The yellow line in Figure 10a shows the area surrounding the ore zone mapped by Kafarskiy et al. (1972). Figure 10b shows the expected location of the dip ore zone and the main ore zone, as described by Kafarskiy et al. (1972) and Sabins & Ellis (2010a).

Jilani, Ahmad & Zuhail (2024) state that the host rocks of the Balkhab copper deposit consists of rhyolite, basalt, and andesitic rocks containing copper minerals, along with sedimentary rocks such as sandstone, pyrite-containing clay, and siliceous clay.

In the Balkhab copper area, sulfide mineralized zones are unconformably located beneath Early-Late Cretaceous sedimentary-volcanic rocks and Late Triassic volcanites (Figure 7). Here, Early Carboniferous metarhyolites intruded the Ordovician and Silurian–Devonian metapelitic–metapsammitic rocks, and simultaneously and/or subsequently, hot hydrothermal solutions associated with the metarhyolites migrated along foliation and fracture zones into both the metapelitic rocks and the metarhyolites (Figure 9a), forming the sulfide mineralized zones.

Copper, lead, and zinc mineralization in the Balkhab copper area occurs within highly fractured, siliceous, and limonitized rocks that contain pyrite zones and sometimes galena. Quartz, malachite, and azurite are observed particularly in oxidized areas, along fracture

zones parallel to schistosity (Figures 11 and 12). Some malachite outcrops are traced for hundreds of meters along the slope (Figure 11a). Iron oxide formations are particularly common in some samples (Figures 12a, b and d). According to Kafarskiy et al. (1972), the dimensions of the mineralized zones are 0.5-2.5 m thick and 180-200 m, sometimes 800 m long (Peters et al., 2011).

Figure 11 Copper outcrops in the Balkhab copper area. a) Schistosity-parallel malachite (Ma), b) Foliation-parallel, folded malachite, c) Malachite zone exposed on the slope, d) Azurite (Az) rich zone



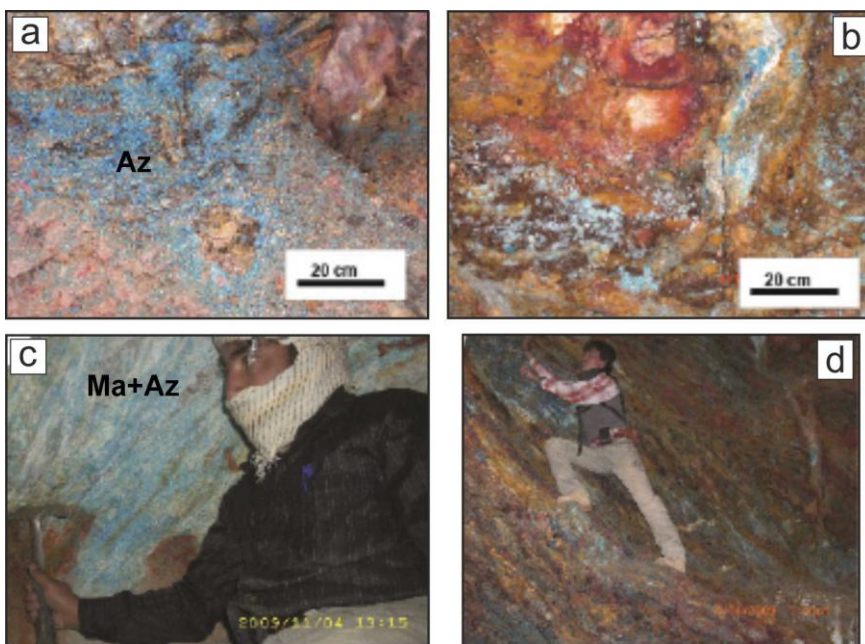
Source: The photographs used in this study were sourced from (Peters et al., 2011), The photographs by Abdul Gaffer, Afghanistan Geological Survey

Jilani, Ahmad & Zuhal (2024) have been stated that in the schistose and massive samples taken from the Mir Sayed Murad area of Balkhab District, Saripul Province - which they identified as metamorphic rocks - the main components observed are feldspar, quartz, copper, amphibole, plagioclase, pyroxene, calcite, sulfur, and

iron oxide, along with minor amounts of pyrite, biotite, and opaque minerals. These researchers found that 11 samples taken from this region contained copper ranging from 0.13% to 27.73%, according to XRF analysis.

Figure 12 Iron-rich mineralized zones in the Balkhab copper area.

a) Brecciated zone containing layered azurite (Az) and red iron-stained oxide minerals, b) Red stained iron oxide zone surrounded by copper oxides, c) Malachite (Ma) and azurite extending parallel to schistosity in metariolites, d) Interlayered malachite and red-spotted mineralized zone



Source: The photographs used in this study were sourced from Peters et al. (2011), The photographs by Abdul Gaffer, Afghanistan Geological Survey

Kafarskiy et al. (1972) reported that in the Balkhab copper area, grid-type sampling revealed, through spectral analysis, 0.02–1 wt% Cu and 0.02–0.07 wt% Zn, and through chemical analysis, 0.25–0.71 wt% Cu and 0.07 wt% Zn along with tin and arsenic.

These researchers found, based on trench sampling, 0.02–1 wt% Cu by spectral analysis and 0.19–1.34 wt% Cu by chemical analysis.

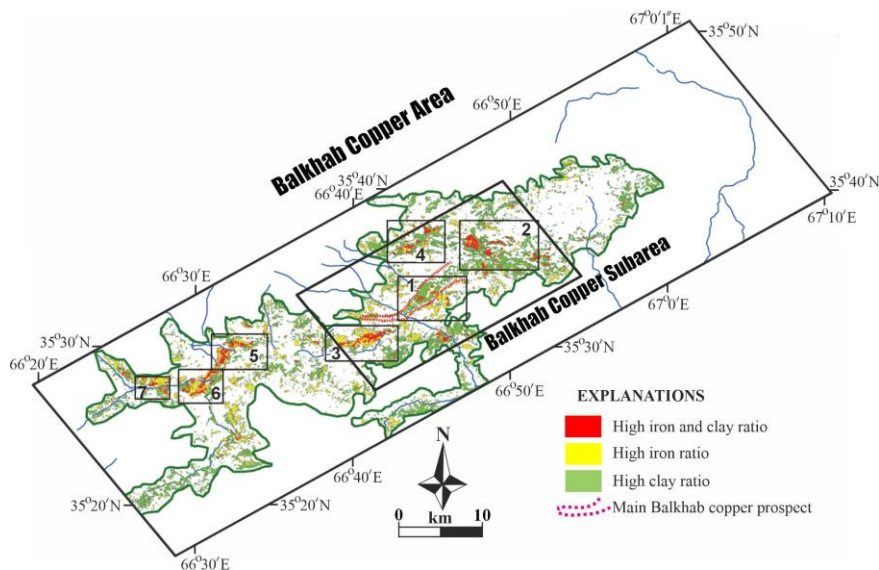
According to Peters et al. (2011), the copper mineralization in the Balkhab copper area consists of a deformed and faulted rock containing silicified limonite, measuring 4,000–5,000 m in length and 300–400 m in width. This rock contains dense malachite, azurite, pyrite, and sometimes chalcopyrite, bornite, and galena in at least four areas, and contains 0.25–1.34% Cu by weight. The geochemical samples collected by the Afghanistan Geological Survey in the Balkhab copper area contain 11,000 ppm Cu, 1,900–6,890 ppm Zn, 5,288 ppm Pb, 1,987 ppm Co, 110–3,939 ppm (up to 155,000 ppm) As, and 500–1,000 ppm P (Peters et al., 2011).

The Balkhab copper deposit exhibits geological features very similar to Kuroko or bimodal-felsic volcanic massive sulfide (VMS) deposits, or a Noranda-type VMS deposit, also referred to as a felsic-intermediate volcanic type deposit (Peters et al., 2007). Typical rocks associated with Kuroko or bimodal-felsic VMS deposits are volcanoclastic rocks, lava flows, felsic lava domes, breccia, and layered sedimentary rocks. Kuroko or bimodal-felsic VMS deposits form towards the more felsic crests of volcanic or volcanic-sedimentary sequences. The rock types and geological setting in the Balkhab copper field indicate that the Balkhab copper deposit is a Kuroko or bimodal-felsic VMS deposit (Peters et al., 2011).

Remotely Detected Anomalies in the Balkhab Copper Area

Sabins & Ellis (2010a) mapped ASTER and hyperspectral imagery in the Balkhab copper district and identified several zones where iron and clay minerals are exposed. As seen in Figure 13, these researchers used a mask of upper contact of deformed Paleozoic rocks with overlying horizontal Mesozoic rocks to map the potential host rocks for the Balkhab copper deposit (Peters et al., 2011).

Figure 13 Anomaly zones identified from Landsat Thematic Mapper change patterns in the Balkhab copper area



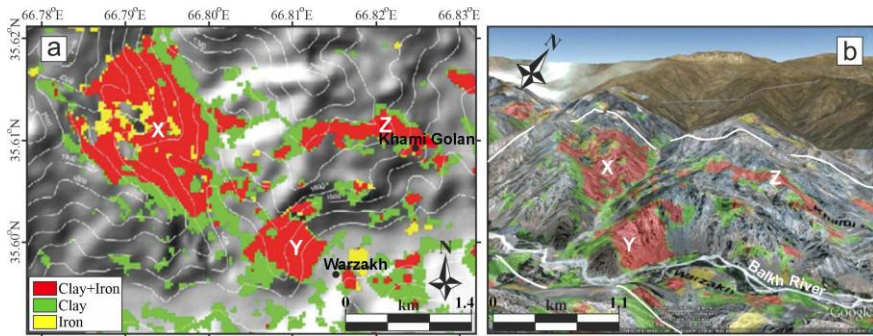
Source: (Sabins & Ellis, 2010a)

In conclusion, seven anomalous zones were identified in the Balkhab copper area (Figure 13). Anomalous zone "1", located in the Balkhab copper subarea, is the main Balkhab copper prospect. Among these anomaly zones, zones 2, 3, and 5 are the most extensive. Anomaly zones 2 and 3 are located in the Balkhab copper subarea (Sabins & Ellis, 2010a; Peters et al., 2011).

Anomaly zone 2 is located on the canyon slopes of the Balkh River and is likely the northeastern extension of the main Balkhab copper prospect (Figures 13 and 14). This zone consists of three main regions (X, Y, Z). These three zones consist of common iron, secondary iron minerals plus clay, and other alteration minerals and clay (Figure 14). Zone X measures 1.5 km - 1 km (length-width), zone Y measures 500 m - 500 m, and zone Z measures 1 km - 200 m. In Figure 14, the green color indicates secondary iron minerals plus clays and other alteration minerals. The red color indicates iron

plus secondary iron minerals plus clays and other alteration minerals (Sabins & Ellis, 2010a; Peters et al., 2011).

Figure 14 Images of anomaly zone 2 in the Balkhab copper subarea, Saripul Province. a) Landsat Thematic Mapper alteration pattern on digital elevation model and contour map. b) Alteration patterns rendered on the IKONOS image. The view is from south of the Balkhab River to northwest. The white outline is the outline of anomaly zone 2 in Figure 13



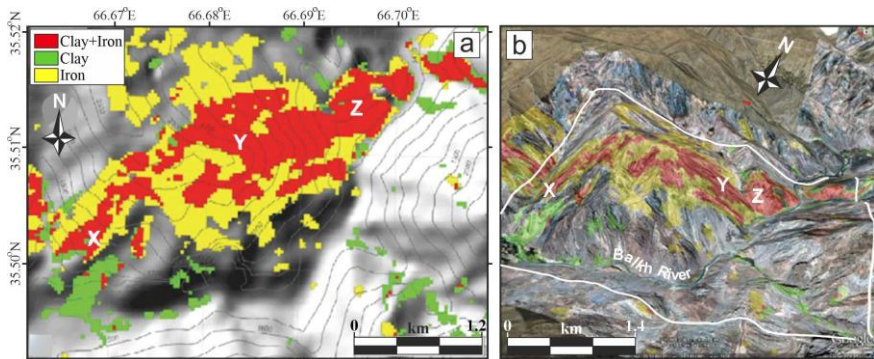
Source: (Sabins & Ellis, 2010a) and (Peters et al., 2011)

Anomaly zone 3 is located southwest of the Balkhab copper subarea (Figure 13). This zone, located on the northern slopes of the Balkh River canyon, is 3 km long and 1 km wide, and consists of clays with secondary iron minerals and other alteration minerals (Figure 15). Anomaly zone 3 is likely a folded or faulted extension of the Balkhab copper mineralization system. In Figure 15, the green color indicates secondary iron minerals plus clays and other alteration minerals. The red color indicates iron plus secondary iron minerals plus clays and other alteration minerals (Peters et al., 2011).

Anomaly zone 5 is located northwest of the Balkhab copper area and 25 km west of Balkhab district (Figure 13). This zone consists of two large areas, approximately 2 km long and 1 km wide, on the northern slopes of the Balkh River canyon (Figure 16b). In Figure 16, the green color indicates secondary iron minerals plus

clays and other alteration minerals. The red color indicates iron plus secondary iron minerals plus clays and other alteration minerals (Sabins & Ellis, 2010a; Peters et al., 2011).

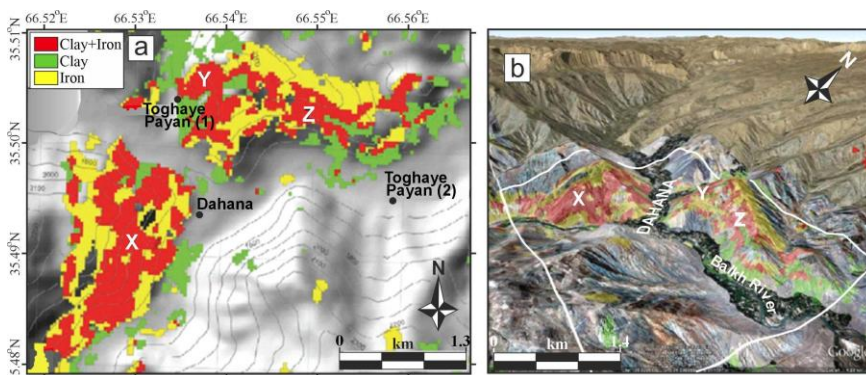
Figure 15 Images of anomaly zone 3 in the Balkhab copper subarea, Saripul Province. a) Landsat Thematic Mapper alteration pattern on digital elevation model and contour map. b) Alteration patterns rendered on the IKONOS image. The view extends from south of the Balkhab River to the northwest. The white outline is the outline of anomaly zone 3 in Figure 13



Source: (Sabins & Ellis, 2010a) and (Peters et al., 2011)

Sabins & Ellis (2010a) determined that, based on the seven anomaly zones they identified in the Balkhab copper area and the Balkhab copper subarea, there are three mineralized systems in the Balkhab copper area. The first of these extends along anomaly zones 1, 2, and 3; the second extends along anomaly zones 5, 6, and 7. The third mineralized system is anomaly zone 4.

Figure 16 Anomaly zone 5 images in Balkhab copper subarea, Saripul Province. a) Landsat Thematic Mapper alteration pattern on the digital elevation model and contour map. b) Alteration patterns mapped onto the IKONOS image. The view is northwest along the Balkhab River. The white outline is the outline of anomaly zone 5 in Figure 13.



Source: (Sabins & Ellis, 2010a) and (Peters et al., 2011)

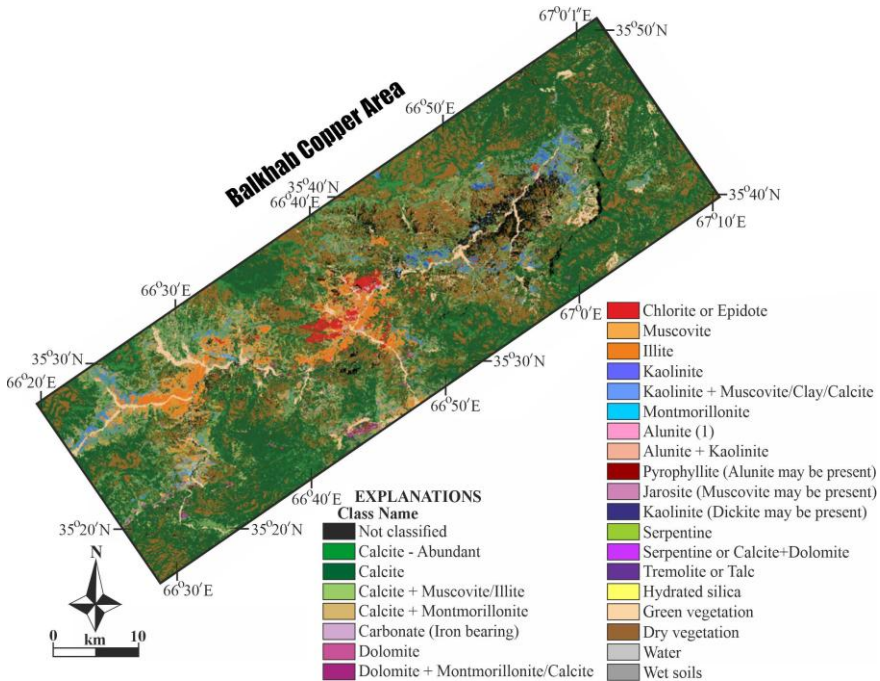
Some Mineral Occurrences Observed in the Balkhab Copper Area

Hoefen & Johnson (2011), using spectroscopic methods, identified a wide variety of minerals exposed at the surface based on the analysis of HyMap imaging spectrometer data from the Balkhab copper area. Although these mineral occurrences may represent minerals hosted within the rocks themselves, they may also indicate a potential for the corresponding mineral deposits.

In Figure 17, a thematic map of carbonates, phyllosilicates, sulfates, altered minerals, and other materials in the Balkhab copper area, created using HyMap data, is shown. As seen in Figure 17, carbonate mineral groups outcrop over a wide area in the Balkhab copper area. Pure muscovite or illite is observed over extensive areas in the central and western parts of the river valley. Kaolinite is found particularly in the central and northwestern parts of the Balkhab

copper area. Large chlorite or epidote zones are located in the central river basin in the western and southwestern parts of the Balkhab copper area. Montmorillonite is generally concentrated in the river valleys (Hoefen & Johnson, 2011).

Figure 17 Map of carbonates, phyllosilicates, sulfates, altered minerals, and other materials derived from HyMap data in the Balkhab copper area

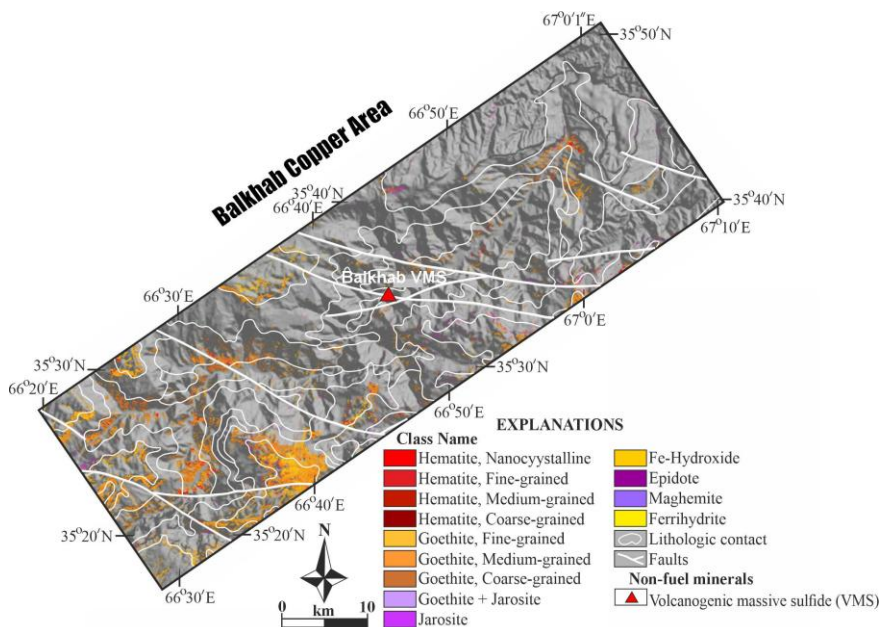


Source: (Hoefen & Johnson, 2011)

The Balkhab copper area contains distinct localized hematite zones in the Ordovician and Late Cretaceous units in the western, southwestern, east-central, and eastern parts of the region (Figure 18). The redstone lithologies described by (Abdullah & Chmyriov, 1977; Doebrich et al., 2006) in the Late Cretaceous units are consistent with the HyMap mineralogical determinations. Hematite

is generally located within or near goethite or Fe-hydroxide zones (Hoefen & Johnson, 2011).

Figure 18 Map of iron oxide and hydroxide distribution in the Balkhab copper area derived from HyMap data



Source: (Hoefen & Johnson, 2011)

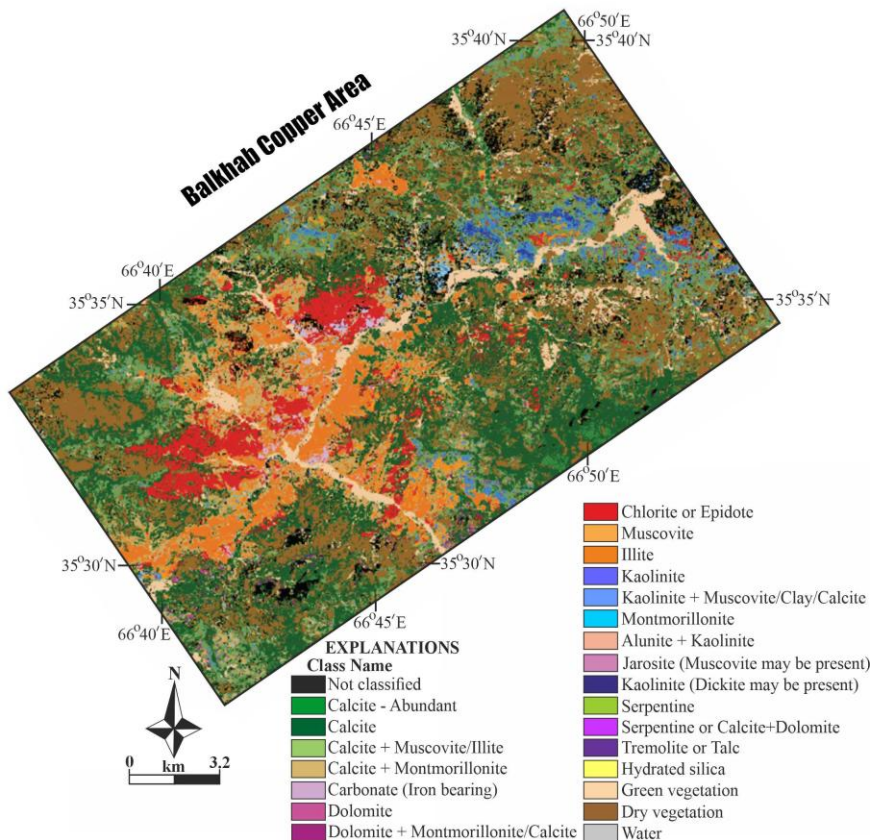
Pixels showing a goethite/Fe-hydroxide signal exhibit a wider distribution compared to hematite and are concentrated mainly in the western and southern parts of the Balkhab copper area (Figure 18). Two distinct goethite–Fe-hydroxide anomaly fields (35°23'57" N – 66°38'49" E; 35°24'06" N – 66°31'08" E) were identified in the central western region (Hoefen & Johnson, 2011).

Jarosite was located approximately 1.9 km south of the Balkhab mine site (Figure 17 and 18). Additional jarosite is distributed at lower concentrations in the western part of the Balkhab copper area. Also, epidote has been mapped in spatially distinct

clusters in the north-central and southwestern margins of the Balkhab copper area (Hoefen & Johnson, 2011).

Figure 19 presents the HyMap MICA analysis output for the 2 μm spectral materials for the Balkhab copper subarea.

Figure 19 Map of carbonate, phyllosilicate, sulfate, alteration minerals and other materials from HyMap data in the Balkhab copper subarea



Source: (Hoefen & Johnson, 2011)

In Figure 19, these spectral materials include clays, carbonates, sulfates, altered minerals, and other spectral phases. Carbonate groups are quite widespread in the Balkhab copper

subarea. Pixels classified as muscovite/illite form broad, continuous zones along the river valley, particularly in the central and southwestern regions. Kaolinite occurs as small but distinct clusters in the south-central and northwestern regions (Hoefen & Johnson, 2011).

As seen in Figure 19, chlorite-epidote group minerals have been identified in large areas concentrated in the central river basin west and southwest of the Balkhab copper subarea (35°34'46" N – 66°44'01" E; 35°32'13" N – 66°41'03" E). Montmorillonite is generally found in localized clusters in the river valleys in the center of the Balkhab copper subarea. Jarosite and hydrated silica minerals occur in close proximity (35°33'32" N – 66°45'24" E) (Hoefen & Johnson, 2011).

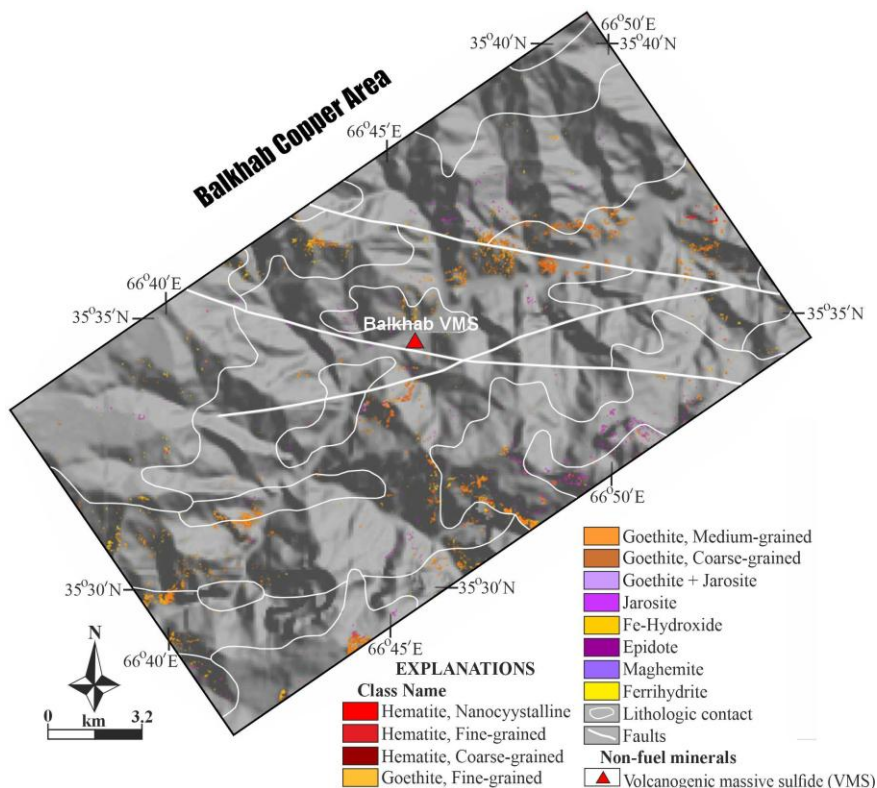
Figure 20 shows the distribution of iron oxide and hydroxide minerals identified from HyMap data in the Balkhab copper subarea. Iron oxide and hydroxide minerals are not common in this subarea. However, small goethite occurrences have been identified throughout the subarea (Hoefen & Johnson, 2011).

Conclusions and Recommendations

The Balkhab copper area is located in northern Afghanistan on the Afghan–Tajik Platform, which represents the Eurasian Plate, within the boundaries of Balkhab District of Saripol Province, Kishindih District of Balkh Province, and Dara-i-Suf District of Samangan Province. Based on previous studies, the following results have been obtained for the Balkhab copper area. The main Balkhab copper area covers 1,858 km², while the Balkhab copper sub-area covers 321 km².

In the Balkhab copper area, Paleozoic lithologies are unconformably overlain by Mesozoic metasedimentary rocks and are intruded by Mesozoic metaplutonic and metavolcanic rocks.

Figure 20 Map of iron oxide and hydroxide distribution in the Balkhab copper subarea obtained from HyMap data



Source: (Hoefen & Johnson, 2011)

The basement rocks, which display low-grade metamorphic characteristics, are represented in the region by Ordovician–Silurian metaclastic rocks and metacarbonates, Early Carboniferous (Mississippian) metavolcanic and metasedimentary rocks, and Early to Late Permian metacarbonates and metaclastics.

South of the Balkh River, these basement rocks are tectonically overlain by Early Carboniferous ophiolites. To the north of the Balkh River, they are cut by Late Triassic granite porphyries. Late Cretaceous units are observed throughout the entire Balkhab

copper area. These are overlain by Late Cretaceous–Paleocene and Early Miocene formations.

In the eastern part of the Balkhab copper area, Late Triassic andesitic lavas overlying Ordovician lithologies are unconformably overlain by Early–Middle Jurassic, Late Jurassic, and Early Cretaceous lithologies. Late Cretaceous units are observed throughout the entire Balkhab copper area. These are overlain by Late Cretaceous–Paleocene and Early Miocene formations.

In the Balkhab copper area, zones of copper-sulfide minerals are observed within or near quartzofeldspathic rocks (felsic volcanic rocks). Most of the quartzofeldspathic rocks contain pyrite, chalcopyrite, and bornite. In the Balkhab copper area, sulfide-mineralized zones occur unconformably beneath the Early–Late Cretaceous sedimentary–volcanic rocks and the Late Triassic volcanites. Here, the Early Carboniferous metarhyolites intruded and emplaced into the Ordovician and Silurian–Devonian metapelitic–metapsammitic rocks, simultaneously with this and/or subsequently, hot hydrothermal fluids associated with the metarhyolites migrated along foliation and fracture zones, penetrating both the metapelitic rocks and the metarhyolites, and forming the sulfide-mineralized zones.

The Balkhab copper deposit is characterized as a Kuroko-type or bimodal-felsic volcanogenic massive sulfide (VMS) deposit. The copper mineralization in the Balkhab copper area occurs within a silicified, limonite-bearing zone that is 4,000–5,000 m long and 300–400 m wide. This zone contains abundant malachite, azurite, pyrite, and occasionally chalcopyrite, bornite, and galena. Quartz, malachite, and azurite occur along fracture zones parallel to the schistosity, particularly in oxidized areas. Geochemical samples collected by the Afghanistan Geological Survey contain concentrations of 11,000 ppm Cu, 1,900–6,890 ppm Zn, 5,288 ppm

Pb, 1,987 ppm Co, 110–3,939 ppm (up to 155,000 ppm) As, and 500–1,000 ppm P.

The Late Triassic granite porphyries exhibit propylitic alteration, and these rocks, which contain continuous quartz–pyrite veins throughout, show trace amounts of valuable base metals.

Coal occurrences are observed in two separate areas in the northeastern part of the Balkhab copper area. The base of the coal sequences lies within Late Cretaceous lithologies, while the upper part of the sequences is mostly traced near the base of the Late Cretaceous–Paleocene lithologies.

Based on previous studies, the main deposit types in the Balkhab copper area are volcanogenic massive sulphide (VMS) deposits including oxide copper ores, coal deposits and possible granite-associated gold deposits. Additionally, the Balkhab copper area contains a number of anomalous or mineralized areas (iron, muscovite, kaolinite, illite, montmorillonite, chlorite, epidote and carbonate minerals) in addition to the main Balkhab copper prospect in the subarea.

Previous studies on stratigraphy, tectonism, metallic ore, industrial raw materials, energy resources and metamorphism in the main Balkhab copper area and Balkhab copper subarea have been based on large-scale geological mappings (1:500,000- (Kafarskiy et al., 1972; Abdullah & Chmyriov, 1977), 1:2,000,000- (ESCAP, 1995), 1:800,000- (Doebrich et al., 2006), 1:300,000- (Hoefen & Johnson, 2011), 1:200,000- (Peters et al., 2011)) and, in general, remote sensing. In previous studies available, studies on the amount of metallic ore (such as Cu, Zn, As, Co, Pb) were obtained from grid sampling, trench sampling, limited surface samplings, open pit excavations, old tunnels - galleries and probably limited and unsystematic drilling core samples in the region. Studies on the type and quantity of industrial raw materials (such as muscovite,

kaolinite, illite, montmorillonite, chlorite, epidote and carbonate) have probably been obtained through limited surface samplings and remote sensing. Coal-related investigations consist of large-scale mapping, limited surface sampling, and data obtained from galleries.

Based on previous studies, and considering the extent and thickness of their occurrences, this region appears to be highly rich in metallic ore, industrial raw materials, and coal-related energy resources. Therefore, it is recommended that the following studies be carried out in the region regarding metallic ore, industrial raw materials and energy resources.

Initially, a 1:10,000 scale geological map of the Balkhab copper area should be prepared and systematic sampling should be carried out. In the region, 1:5,000-scale and, if necessary, 1:1,000-scale geological maps should be prepared for the areas containing metallic mineralizations, coal-related energy raw materials, and industrial raw materials.

Detailed petrographic, petrochemical, and mineral chemistry studies should be carried out on the collected samples. In particular, geochronological analyses should be conducted on the metamagmatic and magmatic rocks to determine their geological ages, and on the metallic ores to determine the age of mineralization.

As a result of these studies, systematic drilling and geophysical investigations should be carried out at the identified locations for the detected metallic ores, industrial raw materials, and energy raw materials.

References

Abdullah, S., & Chmyriov, V. M. (1977). *Geological map of Afghanistan: Kabul, Afghanistan*. Ministry of Mining and Industry of Democratic Republic of Afghanistan, scale 1:500,000.

Abdullah, S., Chmiriov, V. M., Stazhilo-Alekseev, K. F., Dronov, V. I., Gannan, P. J., Rossovskiy, L. N., . . . Malyarov, E. P. (1977). *Mineral resources of Afghanistan*. Republic of Afghanistan, Ministry of Mines and Industries, Afghanistan Geological and Mines Survey, 419 p.

Afghanistan Copper Mines. (2017). Retrieved Ekim 10, 2025, from Moore Afghanistan Web sitesi: <https://afghanistan.moore-global.com/MediaLibsAndFiles/media/afghanistan.moore-global.com/files/Investment-Opportunities/6-Afghanistan-Copper-Mines.pdf>

Afzali, A. O. (2024). Kabil Bloğu'ndaki Metamorfik ve Metamagmatik Kayaçların Petrolojisi ve Jeokimyası, Kabil, Afganistan. *Doktora Tezi, Konya Teknik Üniversitesi, Lisansüstü Eğitim Enstitüsü*, 390 s. Konya, Türkiye.

Ambraseys, N., & Bilham, R. (2003). Earthquakes in Afghanistan. *Seismological Research Letters*, 74(2), 107-123.

Andritzky, G. (1967). Bau und Entstehungsgeschichte des Altkristallin-Keils von Kabil (Afghanistan) und seiner Randzonen. *Geologisches Jahrbuch*, 84, 617-636.

Bohannon, R. G. (2010). Geologic and Topographic Maps of the Kabil North 30' × 60' Quadrangle. Afghanistan. *U.S. Geological Survey*, 1-34.

Boulin, J. (1990). Neocimmerian events in central and western Afghanistan. *Tectonophysics*, 175(4), 211-268.

Boulin, J. (1991). Structures in Southwest Asia and evolution of the eastern Tethys. *Tectonophysics*, 196, 211-268.

Brookfield, M. E., & Hashmat, A. (2001). The geology and petroleum potential of the North Afghan platform and adjacent areas (northern Afghanistan, with parts of southern Turkmenistan, Uzbekistan and Tajikistan). *Earth Science Review*, 55(1), 41-71.

Brookfield, M. E., & Hashmat, A. (2001). The geology and petroleum potential of the North Afghan platform and adjacent areas (northern Afghanistan, with parts of southern Turkmenistan, Uzbekistan and Tajikistan). *Earth-Science Reviews*, 55, 41-71.

Collet, S., Faryad, S. W., & Mosazai, A. M. (2015). Polymetamorphic evolution of the granulite facies Paleo-Proterozoic basement of the Kabil Block, Afghanistan. *Mineralogy and Petrology*, 1-22.

Crone, A. J. (2007). Earthquakes Pose a Serious Hazard in Afghanistan. *USGS Fact Sheet, FS-2007-3027*, 1-4.

Doeblich, J. L., Wahl, R. R., Ludington, S. D., Chirico, P. G., Wandrey, C. J., Bohannon, R. G., . . . Younusi, M. O. (2006). *Geologic and mineral resources map of Afghanistan*. U.S. Geological Survey Open-File Report 2006-1038.

ESCAP. (1995). *Geology and mineral resources of Afghanistan*. Atlas of Mineral Resources of the Economic and Social Commission for Asia and the Pacific Region (ESCAP), New York, 12, 85pp.

Hoefen, T. M., & Johnson, M. R. (2011). Analysis of Imaging Spectrometer Data for the. In S. G. Peters, T. V. King, T. J. Mack, & M. P. Chornack (Eds.), *Summaries of Important Areas for Mineral Investment and Production Opportunities of Nonfuel Minerals in Afghanistan, Chapter: 04B*. US Geological Survey.

Jilani, H. G., Ahmad, R. F., & Zuhal, F. (2024). The Minerals That Make Up the Eastern Part of the Balkhab Copper Mine and Its Nearby Rocks. *American Journal of Geospatial Technology*, 3(1), 76-82.

Kafarskiy, A. K., Stazhilo-Aleksee, K. F., Pyzhyanov, I. V., Achilov, G. S., Gorelov, A. I., Bezulov, G. M., & Gazanfari, S. M. (1972). The geology and minerals of the Western Hindu Kush and the eastern part of the Bande-Turkestan: Kabul. Department of Geological and Mineral Survey, scale 1:500,000, unpublished data, unpaginated.

Kansun, G., & Afzali, A. O. (2022). Geology, Petrographic Characteristics and Tectonic Structure of Paleoproterozoic basement of Kabul Block (North Eastern Afghanistan), Initial Findings. *International Journal of Multidisciplinary Studies and Innovative Technologies (IJMSIT)*, 6 (1), 177-133.

Leven, E. J. (1997). *Permian stratigraphy and fusulinida of Afghanistan with their paleogeographic and paleotectonic implications* (316 ed.). (C. H. Stevens, & D. L. Baars, Eds.) Colorado: Geological Society of America Special Paper.

Mack, T. J., & Chornack, M. P. (2011). Geohydrologic Summary of the Balkhab Copper. In S. G. Peters, T. V. King, T. J. Mack, & M. P. Chornack (Eds.), *Summaries of Important Areas for Mineral Investment and Production Opportunities of Nonfuel Minerals in Afghanistan, Chapter: 04C*. US Geological Survey Open-File Report.

MMAJ. (1998). *Mineral resources map of Asia*. Metal Mining Agency of Japan, 1 sheet and 43 p.

Orris, G. J., & Bliss, J. D. (2002). *Mines and mineral occurrences of Afghanistan*. U.S. Geological Survey Open-File Report 2002-110, 95 p.

Peters, S. G., Ludington, S., Orris, G. J., Sutphin, D. M., Bliss, J. D., & Rytuba, J. J. (2007). Preliminary non-fuel mineral resource assessment of Afghanistan. *US Department of the Interior, US Geological Survey, No: 2007-1214- 045-178*.

Peters, S. G., Mirzad, S. H., Scott, E., & Hubbard, B. E. (2011). Summary of the Zarkashan Copper and Gold Area of Interest. In S. G. Peters, T. V. King, T. J. Mack, & M. P. Chornack (Eds.), *Summaries of Important Areas for Mineral Investment and Production Opportunities of Nonfuel Minerals in Afghanistan, Chapter: 15A*. US Geological Survey Open-File Report 2011–1204.

Peters, S. G., Tucker, R., Gaffer, A., & Hubbard, B. E. (2011). Summary of the Balkhab Copper Area of Interest. In S. G. Peters, T. V. King, T. J. Mack, & M. P. Chornack (Eds.), *Summaries of Important Areas for Mineral Investment and Production Opportunities of Nonfuel Minerals in Afghanistan, Chapter: 04A*. US Geological Survey.

Sabins, F. F., & Ellis, J. E. (2010a). *Landsat analysis of mineral anomalies, Balkhab region, Afghanistan*. Report submitted to Cathay Oil and Gas for U.S. Department of Defense Task Force for Business and Stability Operations, 12 p.

Sabins, F. F., & Ellis, J. E. (2010b). *Coal resources in Balkhab AOI, Remote Sensing Reconnaissance*. Report submitted to Cathay Oil and Gas report for U.S. Department of Defense Task Force for Business and Stability Operations, 14 p.

Sborshchikov, I. M., Loginov, G. S., Dronov, V. I., Bilan, I. K., Cherepov, P. G., & Cherkesov, O. V. (1973). The geology and minerals of Northern Afghanistan: Kabul. Department of Geological and Mineral Survey.

Şengör, A. M. (1984). The Cimmeride orogenic system and the tectonics of Eurasia. *Geological Society of Amerika Special Papers*, 195, 1-74.

Tapponnier, P., Mattauer, M., Proust, F., & Cassaigneau, C. (1981). Mesozoic ophiolites, sutures, and Large-scale tectonic movements in Afghanistan. 52(2), pp. 355-371.

Treloar, P. J., & Izatt, C. N. (1993). Tectonics of the Himalayan collision between the Indian plate and the Afghan block: A synthesis. *Geological Society, London, Special Publications*, 74, 69-87.

Tucker, R. D., Schulz, K. J., & Peters, S. G. (2011). Summary of the Dusar-Shaida Copper and Tin Area of Interest. In S. G. Peters, T. V. King, T. J. Mack, & M. P. Chornack (Eds.), *Summaries of Important Areas for Mineral Investment and Production Opportunities of Nonfuel Minerals in Afghanistan, Chapter: 06A*. US Geological Survey.

SMALLER FORAMINIFERAL ASSEMBLAGE OF THE BASHKIRIAN SUCCESSION IN THE HADİM NAPPE (SOUTHERN TÜRKİYE) AND ITS BIOSTRATIGRAPHIC CORRELATION

**MELİKAN AKBAŞ⁷
CENGİZ OKUYUCU⁸**

Introduction

Since the 1965s, many works dedicated to the Carboniferous foraminifers of the Hadım Nappe, which are mainly focused on fusulinids (e.g. Güvenç, 1965; Monod, 1977; Okuyucu, 1997, 2002; Dzhenchuraeva & Okuyucu, 2007; Kobayashi & Altınır, 2008a, 2008b; Atakul-Özdemir et al., 2011; Kobayashi, 2011; Demirel & Altınır, 2016; Akbaş & Okuyucu, 2021; Akbaş & Okuyucu, 2022a, 2022b). Although there are some studies concerning the Carboniferous smaller foraminifera, biostratigraphic interpretations on Hadım Nappe mainly made based on fusulinid foraminifers by researchers (e.g. Atakul-Özdemir et al., 2011; Demirel & Altınır,

⁷ Asist. Prof. Dr., Konya Technical University, Department of Geological Engineering, ORCID: 0000-0001-8144-8939

⁸ Prof. Dr., Hacı Bayram Veli University, Department of Land Registry and Cadastre, ORCID: 0000-0002-5574-7852

2016; Akbaş & Okuyucu, 2021). Basically, smaller foraminifera of the Devonian, Tournaisian, and Viséan are well documented worldwide, while there are few studies on Bashkirian smaller foraminiferal biostratigraphy without biozonation (see brief in Vachard & Le Coze, 2022). On the other hand, Vachard & Le Coze (2022) reviewed Carboniferous smaller foraminifera and proposed a biozonation that also includes the Bashkirian interval. The fusulinid foraminifers of the Bashkirian successions of the Hadim Nappe were studied in detail by Akbaş (2020) and Akbaş & Okuyucu (2021, 2022a). The authors obtained a rich fusulinid foraminiferal assemblage from the Bashkirian succession of the Hadim Nappe, including fourteen genera and fifty-one species, and based on this assemblage, they subdivided this interval into four local fusulinid biozones; *Plectostaffella jakhensis*-*Plectostaffella bogdanovkensis* Zone, *Pseudostaffella antiqua*-*Pseudostaffella sofronizkyi* Zone, *Staffellaformes staffellaformis*-*Staffellaformes parva parva* Zone, and *Tikhonovichiella tikhonovichi*- *Verella spicata* Zone in ascending order (Akbaş, 2020; Akbaş & Okuyucu, 2021, 2022a).

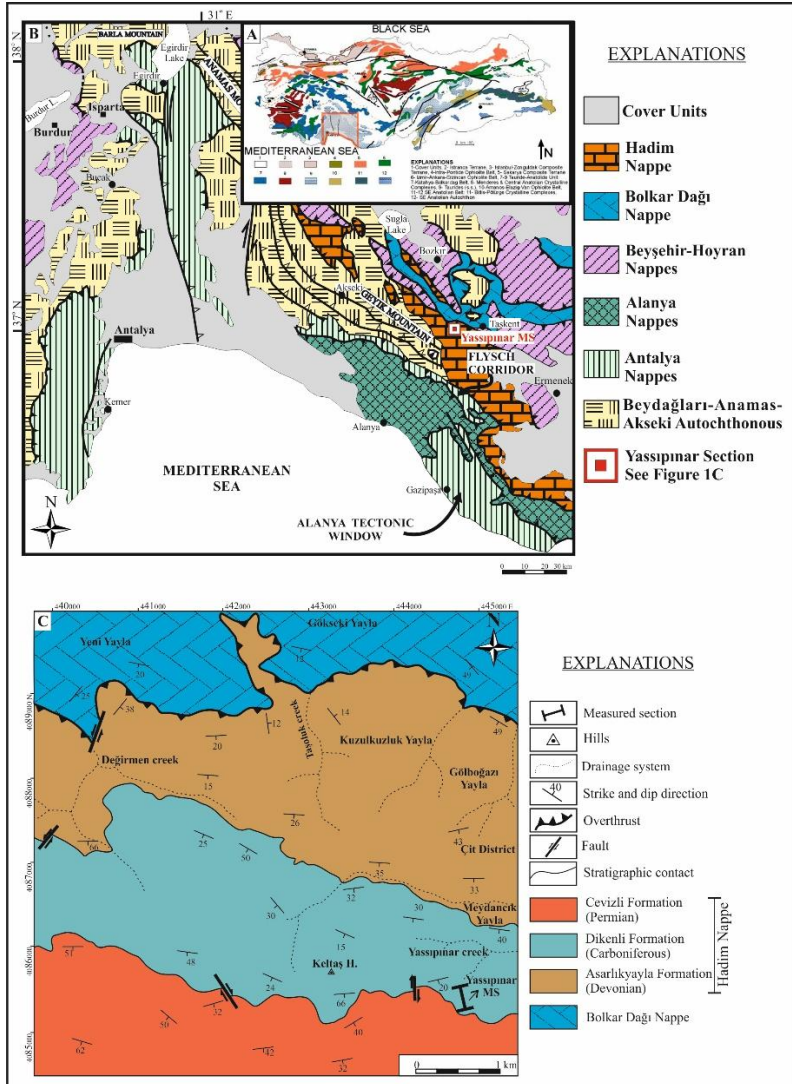
Although fusulinid foraminifers are preferred for biostratigraphy studies of Carboniferous strata after conodont taxa, this interval includes very rich assemblages of smaller foraminifera, which can facilitate easier foraminiferal biostratigraphy studies. For this purpose, within the scope of this study, the thin-sections which were prepared and analysed for fusulinid foraminifers by Akbaş (2020) re-examined for the smaller foraminiferal assemblage of the Bashkirian stage of the Carboniferous succession for the Hadim Nappe.

Geological Setting

Türkiye has been located between the two mega-continents, Laurasia to the north and Gondwana to the south, during its geological history and composed of multiple oceanic and continental

"terrane" with distinct geological features. As a result of many continental fragments from these mega-continentes were rifted off from the main body and amalgamated with each other (Şengör & Yılmaz, 1981; Göncüoğlu, 2010) (Fig. 1A). The Tauride-Anatolide Unit, one of these "terrane" is represented by a continental platform restricted by the Neotethyan Izmir-Ankara-Erzincan Ocean to the north and the Southern Branch of Neotethys to the south, and it comprises of Anatolides, Kütahya-Bolkardağ Belt and Tauride units (Özgül, 1971; Özcan et al., 1990; Göncüoğlu, 2010) (Fig. 1A). The Tauride unit is composed of one autochthonous and several allochthonous units, which are distinguished from each other by their stratigraphic, structural, and metamorphic features (e.g., Blumenthal, 1944, 1951; Brunn, et al., 1971, 1973; Özgül, 1976, 1984, 1997). These autochthonous and allochthonous units of the Tauride unit are settled from north to south, namely Beyşehir-Hoyran Nappes, Bolkar Dağı Nappe, Hadim Nappe, Beydağları-Anamas-Akseki Nappes, Antalya Nappe and Alanya Nappe (Özgül, 1976, 1984) (Fig. 1B, C). Within these allochthonous units, the Hadim Nappe is mainly composed of Middle(?) -Upper Devonian to Upper Cretaceous shallow marine platform type carbonates and siliciclastic rocks (Güvenç, 1977a, 1977b; Monod, 1977; Turan, 1990; Okuyucu & Güvenç, 1997; Özgül, 1997) (Fig. 2). The Hadim Nappe consists of lithostratigraphic units belonging to the Asarlıkaylası formation (Middle-Upper Devonian), Dikenli formation (Carboniferous), Cevizli formation (Permian), Mediova formation (Lower Triassic), Derebucak formation (Upper Triassic-Lower (?) Jurassic), Çamlık formation (Lower Jurassic-Cretaceous), and Zekeriya formation (Upper Cretaceous) in ascending order (Güvenç, 1977b; Monod, 1977; Turan, 1990) (Fig. 2).

Figure 1. A) Terrane Map of Turkey, B) Schematic map showing the Distribution of autochthonous and allochthonous sequences in the area between Western and Central Taurides, C) Geological map of the study area showing the location of the Yassipinar measured section.



Source: A) Göncüoğlu, Kozlu, & Dirik (1997), B) simplified and revised after Özgül (1984), C) simplified and revised after Turan (1990).

Within the Paleozoic succession of the Hadim Nappe, the Asarlıkyaylası formation includes dolomite and dolomitic limestones at the base, and clastic rocks consisting of alternations of sandstone and shale with reefal (biostromal and biohermal) limestones in the upper parts (Monod, 1977; Demirtaşlı, 1984; Turan, 1990; Özgül, 1997) (Fig. 2). The Asarlıkyaylası formation is overlain conformably by the Dikenli formation, which mainly consists of carbonate deposits (limestone, oolitic limestone, dolomite, etc.) and some siliciclastics, with two guide levels: the Turnasian dark shale sequence at the base and the Gzhelian-Sakmarian *Girvanella* limestone sequence at the top (Turan, 1990; Okuyucu & Güvenç, 1997; Özgül, 1997) (Fig. 2). The conformably overlying Permian Cevizli formation consists of algal, foraminiferal/fusulinid, and macro-fossiliferous limestones. The *Girvanella* limestone sequence, which starts from the Gzhelian, forms the base of the Cevizli formation. Additionally, in the lower parts of the formation, there is a quartz arenitic sandstone layer with varying thicknesses regionally, but it remains laterally continuous (Gökten, 1976; Güvenç, 1977a; Monod, 1977; Ayhan & Lengeranlı, 1986; Turan, 1990; Okuyucu, 1997, 2002; Özgül, 1997) (Fig. 2).

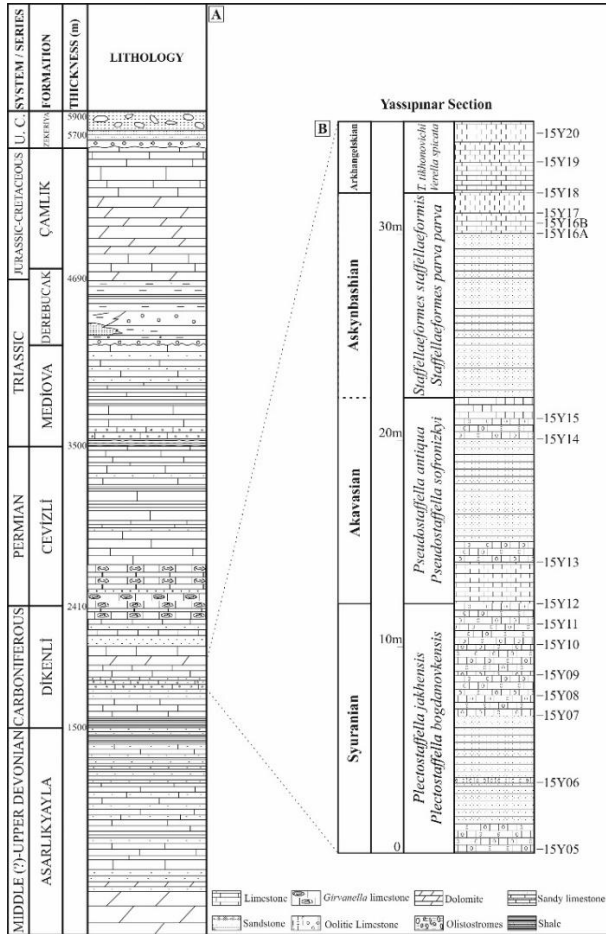
Lithostratigraphy of the Yassıpınar Section

The Yassıpınar section studied by Akbaş (2020) is located about 20 km southwest of the Hadim town (Konya, Türkiye) and mainly consist of shallow marine carbonate deposits bearing a rich and diverse foraminiferal assemblage, and siliciclastic.

The base of the Bashkirian strata of the Yassıpınar section begins with oolitic limestone, which is overlain by quartz arenite sandstone with one limestone interlayer. The overlaying lower-middle part of the section is dominantly characterized by oolitic

limestone and limestone. The middle-upper part of the section is represented by arenite sandstone with rare limestone interlayers. The uppermost part of the section is dominantly composed of limestone (Akbaş, 2020; Akbaş & Okuyucu, 2021, 2022a) (Fig. 2).

Figure 2. A) Generalized columnar section of the Hadim Nappe, B) Lithostratigraphic characteristics, biostratigraphic zonation of the Yassipinar section. Abbreviation: U.C., Upper Cretaceous.



Source: A) modified after Güvenç (1977a, 1977b); Monod (1977); Turan (1990); Okuyucu & Güvenç (1997); Özgül (1997), B) simplified after Akbaş & Okuyucu (2022a).

Biostratigraphy

The fusulinid biostratigraphy of the Bashkirian succession in the Hadim Nappe was thoroughly established, and four fusulinid biozones were identified for this interval by Akbaş (2020) and Akbaş & Okuyucu (2021, 2022a), as previously mentioned. The smaller foraminiferal assemblages defined in this study will be presented under the fusulinid biozones described by Akbaş (2020) and Akbaş & Okuyucu (2022a). According to the analyses of the thin sections, a total of twenty-eight genera and one hundred-two smaller species belonging to these genera were identified in this study.

Smaller foraminifera of the *Plectostaffella jakhensis*-*Plectostaffella bogdanovkensis* zone

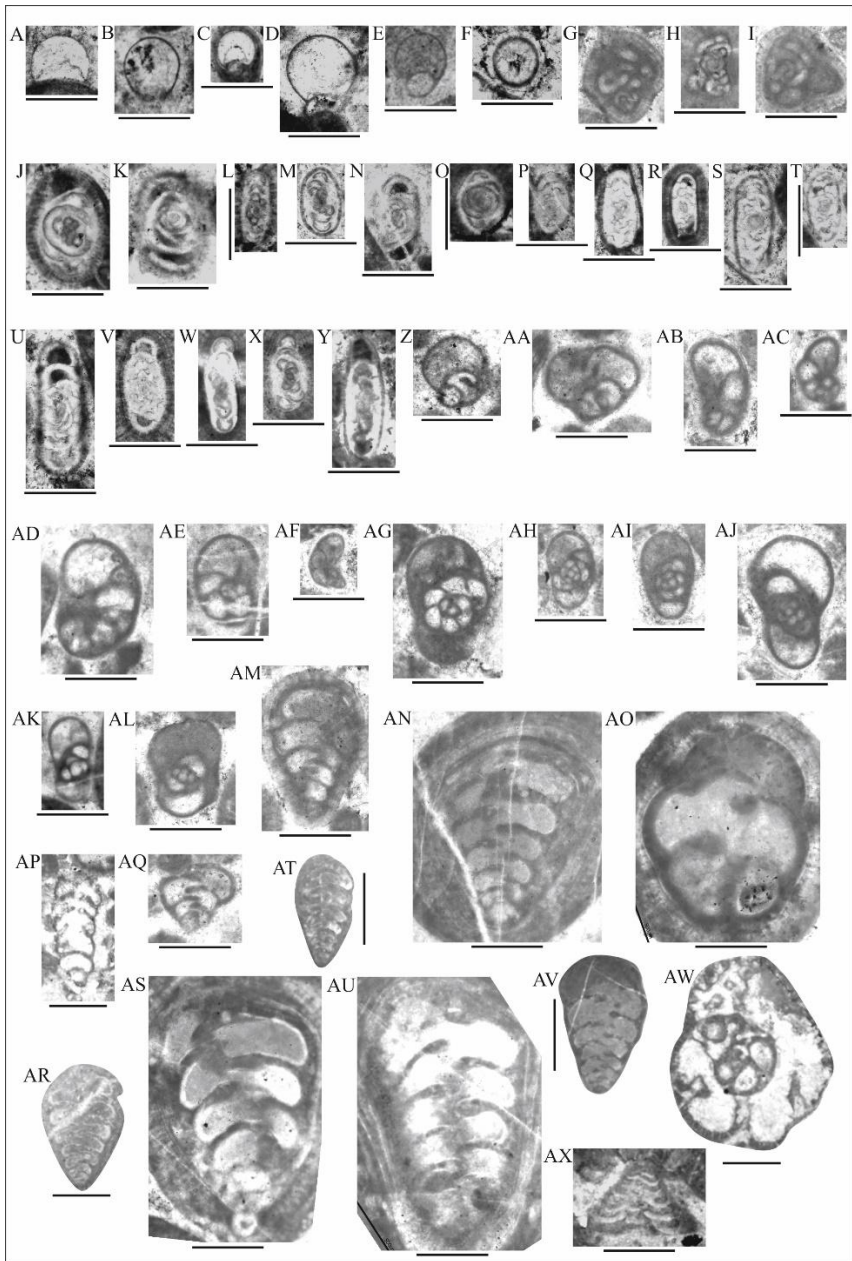
This zone consists mainly of oolitic limestones where the samples 15Y05-15Y11 were collected. These carbonate samples comprise very rich and diverse assemblages of smaller foraminifera, with twenty genera including *Archaeodiscus*, *Asteroarchaediscus*, *Biseriella*, *Bradyina*, *Consobrinellopsis*, *Cribrostomum*?, *Deckerella*, *Diplosphaerina*, *Endothyra*, *Endothyranopsis*, *Eotuberitina*, *Globivalvulina*, *Neoarchaediscus*, *Nodasperodiscus*, *Palaeotextularia*, *Paraarchaediscus*, *Planospirodiscus*, *Pseudoglomospira*, *Radiosphaera*, *Tetrataxis* (Fig. 3). Among them, the taxa that are most notable for their high diversity and abundance are archaeodiscoids, endothyrids, globivalvulinids, and paleotextularids. The entire smaller foraminifera defined in the *Plectostaffella jakhensis*-*Plectostaffella bogdanovkensis* zone of the Yassıpinar section includes the following taxa; *Eotuberitina antiqua*, *E. sphaera*, *Diplosphaerina inaequalis*, *D. sp.*, *Radiosphaera sp.*, *Pseudoglomospira sp.*, *Archaeodiscus postmoelleri*, *A. ex gr. postmoelleri*, *A. stilus*, *A. karreri* subsp. *spira*, *A. ex gr. gissaricus*, *A. sp.*, *Asteroarchaediscus baschkiricus*, *A. rugosus*, *A. rugosimilis*, *A. sp.*, *Neoarchaediscus incertus*, *N. probatus*, *Nodasperodiscus*

planus, *Paraarchaediscus ninae*, *Planospirodiscus?* sp., *Globivalvulina bulloides*, *G. kamensis*, *G. minima*, *G. ex gr. syranica*, *G. sp.*, *Biseriella* sp., *Endothyra explicata*, *E. paraprisca*, *E. polita*, *E. posneri*, *E. ex gr. abramovi*, *Endothyranopsis* sp., *Consobrinellopsis consobrina*, *C. consobrina* subsp. *intermedia*, *Cribrostomum?* sp., *Deckerella* ex gr. *composita*, *Palaeotextularia crassa*, *P. occidentalis*, *P. eogibbosa*, *P. longiseptata*, *P. longiseptata* subsp. *analta*, *P. longiseptata* var. *magna*, *Bradyina* ex gr. *concinna* and *Tetrataxis conica* (Fig. 3).

Globivalvulina bulloides (Fig. 3A) is an important taxon of the lowermost Bashkirian (Syuranian), which was assigned as an index smaller foraminifer for this interval by Vachard (2016) and Vachard & Le Coze (2022). Although the presence of *Globivalvulina bulloides* reported in the upper Serpukhovian strata (e.g. Kulagina & Sinitsyna, 2003; Brenckle & Milkina, 2003; Atakul-Özdemir et al., 2011) it was also commonly known in the lowermost Bashkirian strata (e.g. Groves, 1988; Kulagina et al., 1992, 2000; Atakul-Özdemir et al., 2011). Another globivalvulinids recovered in this study, the *Globivalvulina kamensis* and the *Globivalvulina minima* were also reported in lowermost Bashkirian (Syuranian) strata of the South Urals and Tien-Shan (Kulagina et al., 1992).

Within the archaediscoids foraminifera, defined in the lowermost Bashkirian (Syuranian) strata of the Yassıpinar section, were known in coeval strata from the Hadım Nappe, (Southern Turkey) and South Urals (Russian); *Archaediscus postmoelleri*, (Hadım Nappe, Atakul-Özdemir et al., 2011), *Archaediscus stilus* (South Urals, Kulagina et al., 1992), *Asteroarchaediscus baschkiricus* (Hadım Nappe, Atakul-Özdemir et al., 2011); South Urals, Groves, 1988; Kulagina et al., 1992) and *Asteroarchaediscus rugosus* (Hadım Nappe, Atakul-Özdemir et al., 2011); South Urals, Groves, 1988).

Figure 3. Photomicrographs of the smaller foraminifera assemblages in the *Plectostaffella jakhensis*-*Plectostaffella bogdanovkensis* Zone. A) *Eotuberitina antiqua*, 15Y10-3, B) *E. sphaera*, 15Y10-43, C) *Diplosphaerina inaequalis*, 15Y05-18, D-E) *D. sp.*, D) 15Y05-38, E) 15Y07-3, F) *Radiosphaera sp.*, 15Y10-40, G) *Pseudoglomospira sp.*, 15Y05-5, H) *P. sp.*, 15Y07-6, I) *P. sp.*, 15Y10-9, J) *Archaeodiscus postmoelleri*, 15Y05-26, K) *A. ex gr. postmoelleri*, 15Y10-67, L) *A. stilus*, 15Y05-2, M) *A. karreri subsp. spira*, 15Y05-27, N) *A. ex gr. gissaricus*, 15Y-10-45, O) *A. sp.*, 15Y05-44, P) *Asteroarchaeodiscus baschkiricus*, 15Y05-21, Q-R) *A. rugosus*, Q) 15Y05-30, R) 15Y05-42, S) *A. rugosimilis*, 15Y10-15, T) *A. sp.*, U) *Neoarchaeodiscus incertus*, 15Y10-32, V) *N. probatus*, 15Y05-28, W) *Nodasperodiscus planus*, 15Y05-34, X) *Paraarchaeodiscus ninae*, 15Y05-14, Y) *Planospirodiscus? sp.*, 15Y10-37, Z-AA) *Globivalvulina bulloides*, Z) 15Y05-1, AA) 15Y05-43, AB) *G. kamensis*, 15Y10-27, AC) *G. minima*, 15Y05-33, AD) *G. ex gr. syranica*, 15Y10-49, AE) *G. sp.*, 15Y07-2, AF) *Biseriella sp.*, 15Y10-41, AG) *Endothyra explicata*, 15Y10-8, AH) *E. paraprisca*, 15Y05-37, AI) *E. polita*, 15Y10-60, AJ) *E. posneri*, 15Y10-69, AK) *E. ex gr. abramovi*, 15Y06-1, AL) *Endothyranopsis sp.*, 15Y10-6, AM) *Consobrinellopsis consobrina*, 15Y05-20, AN) *C. consobrina subsp. intermedia*, 15Y06-5, AO) *Cribrostomum? sp.*, 15Y08-1, AP) *Deckerella ex gr. composita*, 15Y05-32, AQ) *Palaeotextularia crassa*, 15Y05-9, AR) *P. occidentalis*, 15Y11-1, AS) *P. eogibbosa*, 15Y08-3, AT) *P. longiseptata*, 15Y10-30, AU) *P. longiseptata subsp. analta*, 15Y09-2, AV) *P. longiseptata var. magna*, 15Y10-51, AW) *Bradyina ex gr. concinna*, 15Y05-24, AX) *Tetrataxis conica*, 15Y10-48. The scale bar is 0.25 mm for A-AO, AQ, AS-AV and AX; 0.5 mm for AP, AR and AW.

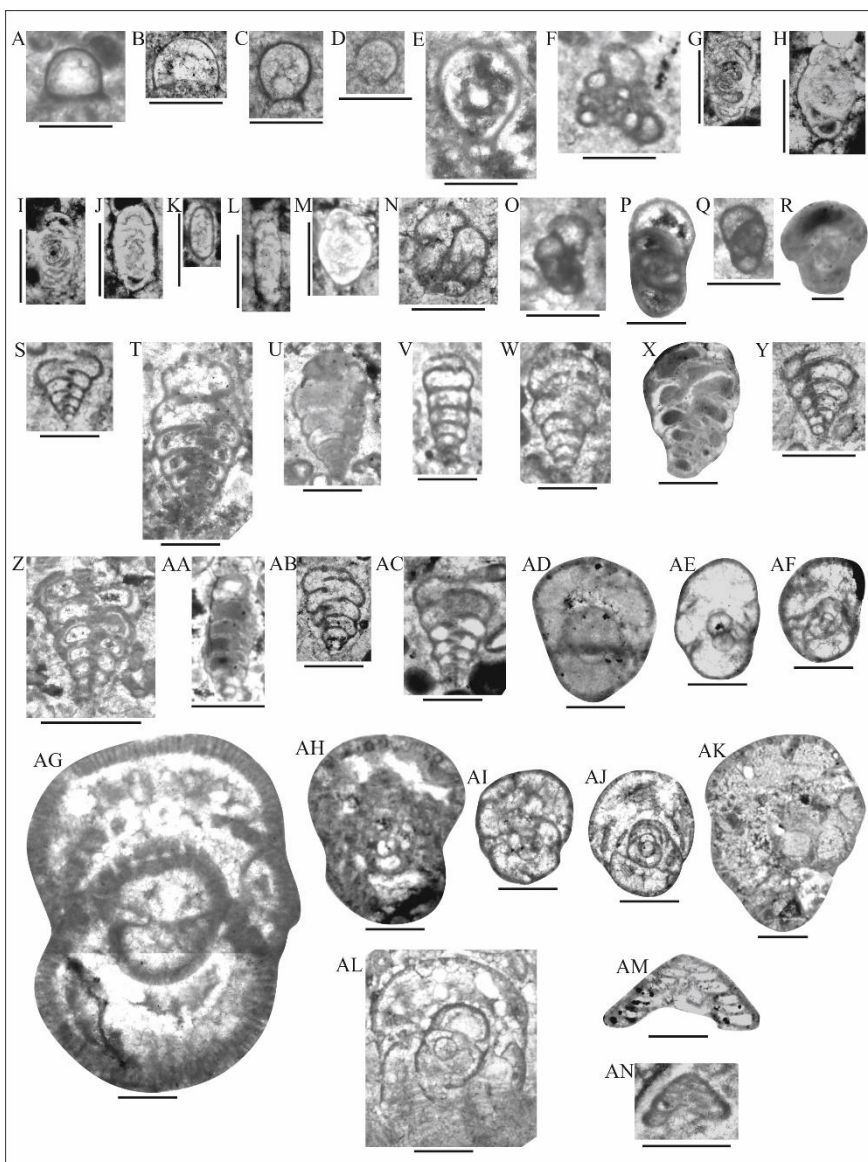


Additionally, *Bradyina* ex gr. *concinna*, *Endothyra paraprisca*, *Nodasperodiscus planus*, and *Palaeotextularia longiseptata* were also reported in the lowermost Bashkirian (Syuranian) strata from South Urals and Tien-Shan (Kulagina et al., 1992).

Smaller foraminifera of the *Pseudostaffella antiqua*-*Pseudostaffella sofronizkyi* zone

This zone is represented by carbonate deposits (oolitic limestone, limestone, etc.) where the samples 15Y12-15Y15 were collected. These carbonates include abundant and diverse smaller foraminiferal assemblages, comprising nineteen genera and forty-nine specimens. The diversity of taxa belonging to the families Bradyinoidea and Palaeotextularioidea increases significantly in this interval (Fig. 4). Essentially, the smaller foraminifera assemblages of this interval, which first occur in this interval, follow as; *Ammovertella* sp., *Archaediscus* ex gr. *subcylindricus*, *A. grandiculus*, *Biseriella parva*, *Bradyina* ex gr. *compressa*, *B. minima*, *B. nautiliformis*, *B. pauciseptata*, *B. pseudonautiliformis*, *B. samarica*, *B. venusta* subsp. *kazakhstanica*, *Cribrostomum posteximium*, *C. stalinogorski*, *Diplosphaerina involuta*, *Endothyra latidorsata*, *Eotuberitina reitlingerae*, *Koskinotextularia cribriformis*, *Neoarchaediscus gregorii*, *N. ovoidea*, *Palaeotextularia brevisseptata*, *P. ex gr. bella*, *P. ex gr. orientalis*, *P. longiseptata* var. *fallax*, *P. simplex*, *Tetrataxis bashkirica*, *T. ex gr. minima* and *Tuberitina* sp. (Fig. 4).

Figure 4. Photomicrographs of the smaller foraminifera assemblages in the *Pseudostaffella antiqua*-*Pseudostaffella sofronizkyi* Zone. A) *Eotuberitina antiqua*, 15Y15-30, B) *E. reitlingerae*, 15Y14-49, C) *E. sphaera*, 15Y15-48, D) *Diplosphaerina involuta*, 15Y15-47, E) *D. sp.*, 15Y15-35, F) *Pseudoglomospira sp.*, 15Y14-11, G) *Archaediscus grandiculus*, 15Y12-12, H) *A.*, 15Y14-22, I) *A. ex gr. subcylindricus*, 15Y12-14, J) *Asteroarchaediscus rugosus*, 15Y12-18, K) *A. sp.*, 15Y13-3, L) *Neoarchaediscus gregorii*, 15Y12-2, M) *N. ovoides*, 15Y14-25, N) *Globivalvulina sp.*, 15Y12-7, O) *Biseriella parva*, 15Y15-31, P) *Endothyra latidorsata*, 15Y15-34, Q) *E. ex gr. posneri*, 15Y15-41, R) *Endothyranopsis sp.*, 15Y14-42, S) *Consobrinellopsis consobrina subsp. intermedia*, 15Y15-36, T) *Cribrostomum posteximium*, 15Y15-8, U) *C. stalinogorski*, 15Y14-52, V) *Deckerella sp.*, 15Y15-24, W) *Koskinotextularia cribriformis*, 15Y12-3, X) *Palaeotextularia brevisseptata*, 15Y14-50, Y) *P. crassa*, 15Y15-40, Z) *P. occidentalis*, 15Y12-19, AA) *P. simplex*, 15Y14-6, AB) *P. longiseptata var. fallax*, 15Y15-46, AC) *P. ex gr. bella*, 15Y14-62, AD) *Bradyina minima*, 15Y14-55, AE) *B. ex gr. compressa*, 15Y14-63, AF) *B. pauciseptata*, 15Y14-61, AG) *B. nautiliformis*, 15Y15-12, AH) *B. pseudonautiliformis*, 15Y14-48, AI) *B.*, 15Y15-14, AJ) *B. venusta subsp. kazakhstanica*, 15Y15-49, AK-AL) *B. sp.*, AM) *Tetrataxis bashkirica*, 15Y14-57, AN) *T. ex gr. minima*, 15Y15-30. The scale bar is 0.25 mm for A-O, Q and AA; 0.5 mm for P, R-Z and AB-AN.



According to Vachard (2016) and Vachard & Le Coze (2022), the last occurrence of *Bradyina cribrostomata* is indicated to the Akavassian substage of the Bashkirian, which corresponds to the *Pseudostaffella antiqua*-*Pseudostaffella sofronizkyi* zone in this study. *Bradyina cribrostomata*, which presence was reported up to

the Akavassian substage by Groves (1988) and Kulagina et al. (1992), was not encountered in this study. The limited studies on the biostratigraphy of smaller foraminifera in the Bashkirian stage, making difficult for correlation to different regions. On the other hand, the presence of an abundant and diverse assemblage of the family Bradyinoidea in this interval shows similarity between the Hadim Nappe (southern Türkiye, this study) and the South Urals and Tien-Shan (Russian Platform, Kulagina et al., 1992). The abundance and diversity of the taxa belonging to the family Palaeotextularioidea in this interval was also reported from South Urals and Tien-Shan by Kulagina et al. (1992). Consequently, the Akavassian substage of the Bashkirian can be assigned as an abundance zone of the smaller foraminifera of the families Bradyinoidea and Palaeotextularioidea.

Smaller foraminifera of the *Staffellaeformes staffellaeformis*-*Staffellaeformes parva parva* zone

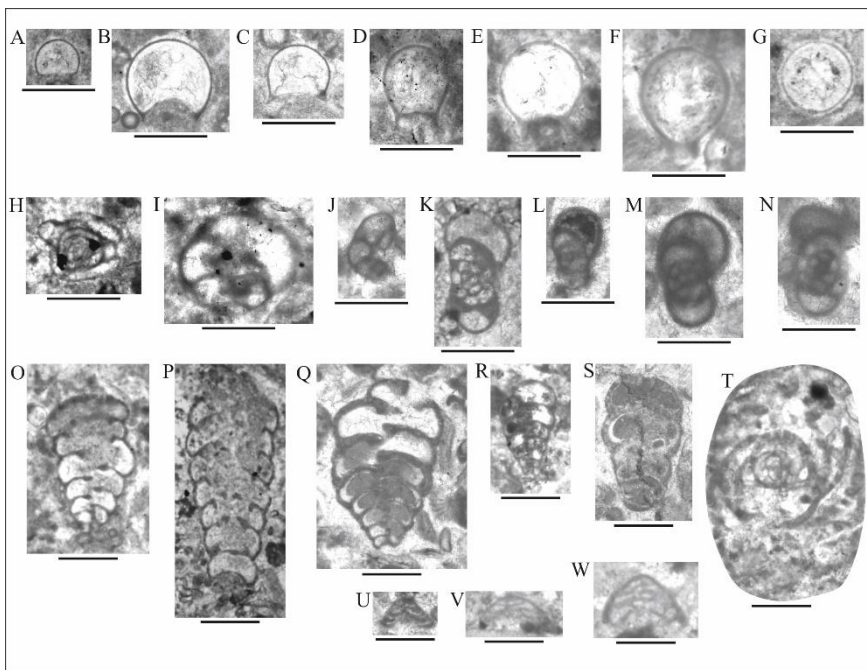
This zone is characterized by siliciclastic rocks at the lower part and limestones at the upper part where the samples 15Y16A, 15Y16B and 15Y17 were collected. *Staffellaeformes staffellaeformis*-*Staffellaeformes parva parva* zone includes relatively less abundant and diverse smaller foraminifera, instead of the previous biozones. The smaller foraminifera assemblage of this zone consists of fourteen genera and twenty-nine specimens, of which only nine specimens occur for the first time in this interval of the Yassıınar section of the Hadim Nappe. These first occurring smaller foraminifera in this zone follow as, *Palaeotextularia* ex gr. *longiseptata*, *Endothyra borealis*, *Radiosphaera* ex gr. *ponderosa*, *R.* sp., *Climacamina aljutovica*, *C.* ex gr. *padunensis* Ganelina, 1956, *Eotuberitina cornuta*, *Bisphaera* sp. and *Tetrataxis* sp. (Fig. 5).

Based on the recovered taxa, the specimens of the families Tuberitinidae, Endothyroidea and Palaeotextularioidea constitute the dominant smaller foraminifera assemblages of the *Staffellaeformes*

staffellaeformis-*Staffellaeformes parva parva* zone (Fig. 5). On the other hand, although the occurrence of the archaedisoids was known up to the Vereian substage of the Moscovian stage (Vachard, 2016; Vachard & Le Coze, 2022), they were not recovered in the upper Bahkirian (Askybashian and Arkhangelskian substages) succession of the Yassıınar section. The other smaller foraminifera fauna, except the dominant foraminifera groups in this zone are as follows, *Ammonvertella* sp. *Biseriella parva*, *Bradyina* sp. *Globivalvulina* sp. *Tetrataxis* ex gr. *minima* and *Tetrataxis* sp. (Fig. 5).

Figure 5. Photomicrographs of the smaller foraminifera assemblages in the *Staffellaeformes*

staffellaeformis-*Staffellaeformes parva parva* Zone. A) *Eotuberitina antiqua*, 15Y16A-20, B) *E. cornuta*, 15Y16A-40, C) *E. reitlingerae*, 15Y16A-31, D) *E. sphaera*, 15Y17-16, E) *E. sp.*, 15Y16A-17, F) *Diplosphaerina* sp., 15Y17-17, G) *Radiosphaera* ex gr. *ponderosa*, 15Y16A-29, H) *Pseudoglomospira* sp., 15Y16A-38, I) *Globivalvulina* sp., 15Y16A-1, J) *Biseriella parva*, 15Y16A-19, K) *Endothyra borealis*, 15Y16A-28, L) *E. parapriscia*, 15Y16B-16, M) *E. posneri*, 15Y16B-13, N) *E. sp.*, O) *Climacammina aljutovica*, 15Y16A-12, P) *C. ex gr. padunensis*, 15Y16A-47, Q) *Palaeotextularia eogibbosa*, 15Y16B-12, R) *P. ex gr. longiseptata*, 15Y16A-24, S) *P. sp.*, 15Y16B-18, T) *Bradyina* sp., 15Y17-9, U) *Tetrataxis* ex gr. *minima*, 15Y16B-24, V) *T. sp.*, 15Y17-4, W) *Tetrataxis* sp., 15Y17-6. The scale bar is 0.25 mm for A-N; 0.5 mm for O-W.



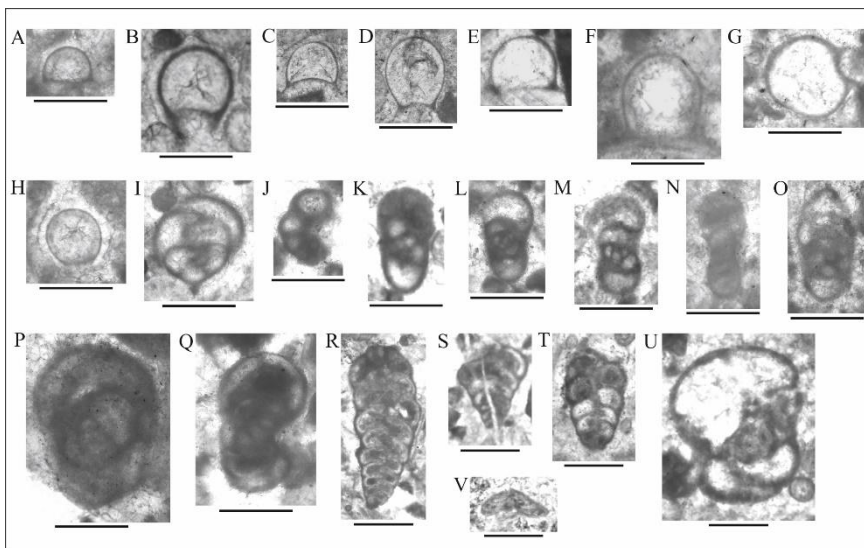
Smaller foraminifera of the *Tikhonovichiella tikhonovichi-Verella spicata* zone

This zone is uniformly composed of fossiliferous limestones where the samples 15Y18, 15Y19 and 15Y20 were collected. *Tikhonovichiella tikhonovichi-Verella spicata* zone is mainly represented by smaller foraminiferal assemblages of the families Tuberitinidae and Endothyroidea. Moreover, smaller foraminifera of the families Palaeotextularioidea, Globivalvulinoidea and Tetrataxoidea are also present in this zone (Fig. 6). The entire smaller foraminiferal fauna of this zone includes fifteen genera and twenty-eight specimens, of which only nine specimens occur for the first time in this interval of the Yassıpınar section. These smaller foraminifera, which occur for the first time in this zone, are as follows; *Endothyra altilis*, *E. perfida* var. *crebra*, *Planoendothyra spirilliniformis*, *Eoendothyranopsis rotayi*, *Bradyina modica*,

Eotuberitina crassa, *E. ex gr. angustata*, *Timanella lata* and *Radiosphaerina* sp. (Fig. 6).

According to Vachard & Le Coze (2022), the lower and upper parts of the uppermost Bashkirian are represented by the first appearance of *Endothyranella* spp. and the last occurrence of *Biseriella parva*, respectively. Additionally, *Biseriella parva* is also reported from the uppermost Bashkirian strata of the Southern Urals by Groves (1988). The presence of *Biseriella parva* in the uppermost Bashkirian strata in the Yassıpinar section supports the argument of Vachard & Le Coze (2022) for this taxon. On the other hand, specimens belonging to the genus *Endothyranella*, which are assigned as index taxa for the base of the uppermost Bashkirian strata by Vachard & Le Coze (2022), were not recovered in the Yassıpinar section.

Figure 6. Photomicrographs of the smaller foraminifera assemblages in the *Tikhonovichiella tikhonovichi*-*Verella spicata* Zone. A) *Eotuberitina antiqua*, 15Y20-13, B) *E. cornuta*, 15Y18-9, C) *E. crassa*, 15Y20-24, D) *E. ex gr. angustata*, 15Y20-27, E) *E. ex gr. reitlingerae*, 15Y19-10, F) *E. ex gr. sphaera*, 15Y20-5, G) *Bisphaera* sp., 15Y18-14, H) *Radiosphaera* sp., 15Y18-2, I) *Globivalvulina* sp., 15Y19-1, J) *Biseriella parva*, 15Y19-22, K) *Endothyra altilis*, 15Y19-7, L) *E. paraprisca*, 15Y19-8, M) *E. perfida* var. *crebra*, 15Y20-14, N) *Planoendothyra spirilliniformis*, 15Y20-12, O) *Timanella lata*, 15Y20-23, P) *Endothyranopsis* sp., 15Y20-2, Q) *Eoendothyranopsis rotayi*, 15Y19-13, R) *Climacammina aljutovica*, 15Y19-26, S) *Palaeotextularia crassa*, 15Y19-24, T) *P. sp.*, 15Y19-12, U) *Bradyina modica*, 15Y19-28, V) *Tetrataxis* sp., 15Y20-29. The scale bar is 0.25 mm for A-Q; 0.5 mm for R-V.



Conclusions

The depositional environment of the shallow marine carbonates of the Carboniferous succession of the Hadim Nappe indicated idealized life conditions for marine microorganisms, which resulted in an abundant and diverse foraminiferal record. Besides the reported abundant and diverse fusulinid assemblages, the Bashkirian succession of the Hadim Nappe also includes a rich and diverse smaller foraminifera fauna. These smaller foraminifera can also be useful for biostratigraphy studies when index fusulinids are lacking and/or restricted.

A total of twenty-eight genera and one hundred-two smaller foraminifera specimens belonging to these genera were obtained from Bashkirian succession of the Yassıpınar section of the Hadim Nappe. The distribution and biostratigraphic consideration of these smaller foraminifera was made under the previously described fusulinid biozones. The prominent smaller foraminifera groups of the *Plectostaffella jakhensis*-*Plectostaffella bogdanovkensis* zone are archaediscoids, endothyrids, globivalvulinids, and

paleotextularids. Within these smaller foraminifera of this zone, especially *Globivalvulina bulloides* and most of the archaedisoids provide a well correlation with the coeval succession of the South Urals and Tien-Shan. The Akavassian substage of the Bashkirian, corresponding to the *Pseudostaffella antiqua*-*Pseudostaffella sofronizkyi* zone, can be assigned as an abundance zone of the smaller foraminifera of the families Bradyinoidea and Palaeotextularioidea related to the diversity of taxa belonging to these families increases significantly in this interval. The dominant smaller foraminifera assemblages of the *Staffellaeformes staffellaeformis*-*Staffellaeformes parva parva* zone mainly belong to the families Tuberitinidae, Endothyroidea and Palaeotextularioidea. The uppermost biozone, the *Tikhonovichiella tikhonovichi*- *Verella spicata* zone, is mainly characterized by abundance of the smaller foraminiferal assemblages belong to the families Tuberitinidae and Endothyroidea. Smaller foraminifera of the families Palaeotextularioidea, Globivalvulinoidea and Tetrataxioidea are also present in the *Tikhonovichiella tikhonovichi*- *Verella spicata* zone. Within these smaller foraminifera assemblages of the *Tikhonovichiella tikhonovichi*- *Verella spicata* zone, the occurrence of *Biseriella parva* in the uppermost Bashkirian strata in the Yassipınar section shows a well correlation with coeval successions of the different regions (e.g., Southern Urals).

References

Akbaş, M. (2020). Foraminiferal biochronology, microfacies analysis and environmental interpretation of Bashkirian-Moscovian (lower and middle Pennsylvanian) successions in the Hadim Nappe (Central Taurides) [Unpublished PhD Thesis]. Konya: Konya Technical University, Institute of Graduate Studies, Department of Geological Engineering.

Akbaş, M., & Okuyucu, C. (2021). Biostratigraphy and taxonomy of fusulinid foraminifera across the Upper Mississippian (upper Serpukhovian)-Lower Pennsylvanian (Bashkirian) successions from the Hadim Nappe, Central Taurides, southern Turkey. *Journal of Paleontology*, 95(3), 476-496. doi:10.1017/jpa.2020.116

Akbaş, M., & Okuyucu, C. (2022a). Fusulinid biozonation of the Bashkirian–Moscovian successions from the Hadim Nappe, central Taurides, southern Turkey. *PalZ*, 96, 517-541. doi:10.1007/s12542-022-00622-w

Akbaş, M., & Okuyucu, C. (2022b). Fusulinid biostratigraphy of the Moscovian-Lower Kasimovian of Hadim Nappe, Central Taurides, southern Turkey. *Geodiversitas*, 44(19), 527-562. doi:10.5252/geodiversitas2022v44a19

Atakul-Özdemir, A., Altıner, D., Özkan-Altıner, S., & Yılmaz, İ. Ö. (2011). Foraminiferal biostratigraphy and sequence stratigraphy across the mid–Carboniferous boundary in the Central Taurides, Turkey. *Facies*, 57(4), 705-730. doi:10.1007/s10347-010-0260-y

Ayhan, A., & Lengeranlı, Y. (1986). Yahyalı-Demirkazık (Aladağlar yöresi) arasının tektonostratigrafik özellikleri. *Jeoloji Mühendisliği Dergisi*, 27, 31-45.

Blumenthal, M. M. (1944). Bozkır güneyinde Toros sıradağlarının serisi ve yapısı. *İstanbul Üniversitesi Fen Fakültesi Mecmuası, Seri B, 9(2)*, 95-125.

Blumenthal, M. M. (1951). Batı Toroslarda Alanya ard ülkesinde jeolojik araştırmalar. *Maden Tetkik ve Arama Enstitüsü Yayınları, Seri D, 5*, 1-194.

Brenckle, P. L., & Milkina, N. V. (2003). Foraminiferal timing of carbonate deposition on the Late Devonian (Famennian)-Middle Pennsylvanian (Bashkirian) Tengiz platform, Kazakhstan. *Rivista Italiana di Paleontologia e Stratigrafia, 109*, 131-158. doi:10.13130/2039-4942/5498

Brunn, J. H., Argyriadis, I., Marcoux, J., Monod, O., Poisson, A., & Ricou, L. (1973). Antalya'nin ofiyolit naplarının orijini lehinde ve aleyhinde kanıtlar [Evidence of the origin of the Ophiolite Nappes of Antalya]. *Cumhuriyetin 50. Yili Yerbilimleri Kongresi, Mineral Research and Exploration Publications*, 58-69.

Brunn, J. H., Dumont, J., De Graciansky, P. C., Gutnic, M., Juteau, T., Marcoux, J., . . . Poisson, A. (1971). Outline of the geology of the western Taurids, In: Geology and history of Turkey. (A. S. Campbell, Ed.) *Petroleum Exploration Society of Libya*, 225-255.

Demirel, S., & Altın, D. (2016). Foraminiferal biostratigraphy and glacioeustatic control on cyclic carbonate microfacies in the Viséan-Serpukhovian boundary beds (Aladağ Unit, Eastern Taurides, Turkey). *Facies, 62*, 1-32. doi:10.1007/s10347-015-0451-7

Demirtaşlı, E. (1984). Stratigraphy and tectonics of the area between Silifke and Anamur, Central Taurus Mountains. In O. Tekeli, & M. C. Göncüoğlu (Ed.), *International Symposium on Geology of the Taurus Belt* (pp. 101-118). Ankara: MTA.

Dzhenchuraeva, A. V., & Okuyucu, C. (2007). Fusulinid Foraminifera of the Bashkirian-Moscovian boundary in the eastern Taurides, southern Turkey. *Journal of Micropalaeontology*, 26, 73-85. doi:10.1144/jm.26.1.73, 2007

Gökten, E. (1976). Silifke yöresinin temel kaya birimleri ve Miyosen stratigrafisi. *Türkiye Jeoloji Kurumu Bülteni*, 19(2), 117-126.

Göncüoğlu, M. C. (2010). *Introduction to the geology of Turkey: geodynamic evolution of the pre-alpine and alpine terranes*. Ankara: MTA Monography series.

Göncüoğlu, M. C., Kozlu, H., & Dirik, K. (1997). Pre-Alpine and Alpine terranes in Turkey: explanatory notes to the terrane map of Turkey. *Ann. Geol. Pays Helleniques*, 37, 515-536.

Groves, J. R. (1988). Calcareous foraminifers from the Bashkirian stratotype (middle Carboniferous, South Urals) and their significance for intercontinental correlations and the evolution of the Fusulinidae. *Journal of Paleontology*, 62, 368-399.

Güvenç, T. (1965). Étude stratigraphique et micropaléontologique du Carbonifère et du Permien des Taurus occidentaux dans l'arrière-pays d'Alanya (Turquie), [Ph.D. dissertation]. Paris: Université de Paris.

Güvenç, T. (1977a). Permian of Turkey. *6th Colloquium of the Geology of Aegean Regions* (pp. 263-282). İzmir: Aegean University.

Güvenç, T. (1977b). Stratigraphie du Carbonifère et du Permien de la Nappe de Hadim. *6th Colloquium of the Geology of Aegean Regions* (pp. 251-261). İzmir: Aegean University.

Kobayashi, F. (2011). Two species of Profusulinella (*P. aljutovica* and *P. ovata*), early Moscovian (Pennsylvanian) fusulines

from southern Turkey and subdivision of primitive groups of the Family Fusulinidae. *Rivista Italiana di Paleontologia e Stratigrafia*, 117(1), 29-37. doi:10.13130/2039-4942/5961

Kobayashi, F., & Altiner, D. (2008a). Fusulinoidean faunas from the Upper Carboniferous and Lower Permian platform limestone in the Hadim Area, Central Taurides, Turkey. *Rivista Italiana di Paleontologia e Stratigrafia*, 114(2), 191-232. doi:10.13130/2039

Kobayashi, F., & Altiner, D. (2008b). Late Carboniferous and Early Permian fusulinoideans in the central Taurides, Turkey: biostratigraphy, faunal composition and comparison. *The Journal of Foraminiferal Research*, 38(1), 59-73. doi:10.2113/gsjfr.38.1.59

Kulagina, E. I., & Sinitsyna, Z. A. (2003). Evolution of the Pseudostaffellidae in the Bashkirian Stage (middle Carboniferous). *Rivista Italiana di Paleontologia e Stratigrafia*, 109, 213-224. doi:10.13130/2039-4942/5503

Kulagina, E. I., Pazukhin, V. N., Nikolaeva, S. V., & Kochetova, N. N. (2000). Biozonation of the Syuran horizon of the Bashkirian Stage in the South Urals as indicated by ammonoids, conodonts, foraminifers and ostracodes. *Stratigraphy and Geological Correlation*, 8, 13-156.

Kulagina, E. I., Rumyantseva, Z. C., Pazukhin, V. N., & Kochetova, N. N. (1992). *Boundary Early–Middle Carboniferous in the Southern Urals and Central Tian-Shan*. Moskva: Rossiiskaya Akademiya Nauk, Uralskoe Otdelenie, Bashkirskii Nauchnyi Tsentr, Institut Geologii.

Monod, O. (1977). *Recherches Geologiques Dans le Taurus Occidental au Sud de Beyşehir (Turquie)* [Ph.D. dissertation]. Paris: Université de Paris Sud.

Okuyucu, C. (1997). Hadim Napı Karbonifer-Permiyen geişı biyostratigrafisi, Yüksek Lisans Tezi. Ankara: Hacettepe Üniversitesi, Fenbilimleri Enstitüsü.

Okuyucu, C. (2002). Toroslarda Anadolu Platformu Karbonifer-Permiyen geisinin mikropaleontolojik incelemesi. Ankara: Hacettepe Üniversitesi, Fen Bilimleri Enstitüsü.

Okuyucu, C., & Güven, T. (1997). Hadim Napı'nda Karbonifer-Permiyen geişı, Girvanella kiretaşı oluřum paleontolojisi. *Yerbilimleri (Geosound)*, 30, 463-473.

Özcan, A., Göncüoğlu, M. C., Turhan, N., Uysal, ř., & řentürk, K. (1990). Late Paleozoic evolution of the Kütahya-Bolkardağı Belt. *METU Journal of Pure and Applied Sciences*, 21(1-3), 211-220.

Özgöl, N. (1971). Orta Torosların kuzey kesiminin yapısal gelişiminde blok hareketlerinin önemi. *Türkiye Jeoloji Kurumu Bülteni*, 14(1), 85-101.

Özgöl, N. (1976). Toroslar'ın bazı temel jeoloji özellikleri. *Türkiye Jeoloji Kurumu Bülteni*, 19, 65-78.

Özgöl, N. (1984). Stratigraphy and tectonic evolution of the Central Taurides. In O. Tekeli, & M. C. Göncüoğlu (Ed.), *International Symposium on Geology of the Taurus Belt* (pp. 77-90). Ankara: MTA.

Özgöl, N. (1997). Bozkır-Hadim-Tařkent (Orta Toroslar'ın kuzey kesimi) dolayında yer alan tektono-stratigrafik birliklerin stratigrafisi. *Maden Tetkik ve Arama Dergisi*, 119, 113-174.

řengör, M. C., & Yılmaz, Y. (1981). Tethyan evolution of Turkey: A plate tectonic approach. *Tectonophysics*, 75, 181-241.

Turan, A. (1990). Toroslar'da Hadim (Konya) ve g neybatısının jeolojisi, stratigrafisi ve tektonik geliřimi, [Doktora Tezi]. Konya: Sel uk  niversitesi, Fen Bilimleri Enstit s .

Vachard, D. (2016). Macroevolution and Biostratigraphy of Paleozoic Foraminifer. In M. Montenari (Ed.), *Stratigraphy & Timescales* (Vol. 1, pp. 257-323). Amsterdam: Elsevier.

Vachard, D., & Le Coze, F. (2022). Carboniferous smaller Foraminifera: convergences and divergences. *Geological Society, London, Special Publications*, 512, 247-326. doi:10.1144/SP512-2020-42

ACADEMIC STUDIES IN GEOSCIENCE

